AD NUMBER

ADB001669

NEW LIMITATION CHANGE

TO

Approved for public release, distribution unlimited

FROM

Distribution authorized to U.S. Gov't. agencies only; Test and Evaluation; 19 Nov 1974. Other requests shall be referred to Air Force Rocket Propulsion Laboratory, Attn: STINFO/DOZ, Edwards AFB, CA 93523.

AUTHORITY

AFRPL ltr, 15 May 1986

Report AFRPL-TR-74-78
Volume I

ALUMINUM HYDRIDE PROPELLANT SHELFLIFE

Final Report For Period December 1970 - July 1974

W. E. Baumgartner

Lockheed Propulsion Company
Redlands, CA 92373

November 1974

Air Force Rocket Propulsion Laboratory
Director of Science and Technology
Air Force Systems Command
Edwards, California 93523

FOREWORD

This report was submitted by Lockheed Propulsion Company, Redlands, California 92373, under Contract F04611-71-C-0018, Job Order No. 305908LM with the Air Force Rocket Propulsion Laboratory, Edwards, California 93523.

This technical report is approved for release and distribution in accordance with the distribution statement on the cover and on the DD Form 1473.

Norman J. Vanderhyde, GS-14
Project Engineer

Robert L. Geisler, GS-14
Chief, Propellant
Development Branch

Charles R. Cooke
Chief, Solid Rocket Division

UNCLASSIFIED

SECURITY CLASSIFICATION OF THIS PAGE (When Data Entered)

REPORT DOCUMENTATION PAGE		READ INSTRUCTIONS BEFORE COMPLETING FORM
1. REPORT NUMBER AFRPL-TR-74-78, Vol I	2. GOVT ACCESSION NO.	3. RECIPIENT'S CATALOG NUMBER
4. TITLE (and Subtitle) ALUMINUM HYDRIDE PROPELLANT SHELFLIFE		5. TYPE OF REPORT & PERIOD COVERED Technical Report - Final Dec 1970 to July 1974
		6. PERFORMING ORG. REPORT NUMBER 532-F
7. AUTHOR(s) W. E. Baumgartner		8. CONTRACT OR GRANT NUMBER(s) F04611-71-C-0018
9. PERFORMING ORGANIZATION NAME AND ADDRESS Lockheed Propulsion Company A Division of Lockheed Aircraft Corporation P.O. Box 111, Redlands, California 92373		10. PROGRAM ELEMENT, PROJECT, TASK AREA & WORK UNIT NUMBERS 305908LM
11. CONTROLLING OFFICE NAME AND ADDRESS Air Force Rocket Propulsion Laboratory Air Force Systems Command Edwards, AFB, California 93523		12. REPORT DATE 30 November 1974 13. NUMBER OF PAGES 90
14. MONITORING AGENCY NAME & ADDRESS(if different from Controlling Office)		15. SECURITY CLASS. (of this report) UNCLASSIFIED 15a. DECLASSIFICATION/DOWNGRADING SCHEDULE N/A

16. DISTRIBUTION STATEMENT (of this Report)

Distribution limited to U.S. Government agencies only; Test and Evaluation, 19 November 1974. Other requests for this document must be referred to AFRPL(STINFO/DOZ), Edwards, CA 93523

17. DISTRIBUTION STATEMENT (of the abstract entered in Block 20, if different from Report)

Same

18. SUPPLEMENTARY NOTES

19. KEY WORDS (Continue on reverse side if necessary and identify by block number)

Aluminum hydride	Accellerated aging	Service life
Propellant	Chemical aging	
TVOPA	Halpin analysis	
PCDE	Creep failure	
Thermal stability	Scavengers	

20 ABSTRACT (Continue on reverse side if necessary and identify by block number)

The thermal stability and service life capability of an AlH /TVOPA and PCDE based propellants were evaluated relying upon accelerated surveillance tests accompanied by X-ray analyses, off-gas analyses, tensile testing and determination of creep failure distributions. The Halpin statistical cumulative damage analysis principle was implemented for interpreting the creep failure test data.

DD FORM 1 JAN 73 1473 EDITION OF 1 NOV 65 IS OBSOLETE

UNCLASSIFIED

SECURITY CLASSIFICATION OF THIS PAGE (When Data Entered)

Catalytic gas scavengers were shown to extend the 20°C shelflife of AlH /TVOPA propellants to better than 3 years. However, difficulties in assuring close batch-to-batch reproducibility, and noticeable binder degradation at storage temperatures in excess of 20°C cause this propellant to be of questionable merit in military application.

A ballistically optimized PCDE propellant failed within relatively short storage times at moderate temperatures, and the rather premature failure was attributed to a combination of internal gassing and binder polymer degradation. Both deficiencies appear to be associated with residual impurities, or structural irregularities in the prepolymer, and the problem is expected to be overcome by further material development. At higher storage temperatures the PCDE based systems appear to undergo a secondary crosslink process, this phenomenon merits further investigation.

The Halpin statistical cumulative damage analysis approach, which was used to analyze and interpret the creep failure data, was shown to be applicable for assessing the effects of chemical aging upon creep failure distributions and to provide a means for predicting propellant-in-motor service life under given time-temperature-load conditions.

TABLE OF CONTENTS

TABLE OF CONTENTS (Continued)

LIST OF ILLUSTRATIONS

LIST OF ILLUSTRATIONS (Continued)

LIST OF TABLES

(The reverse is blank)

1. INTRODUCTION

1.1 BACKGROUND

There has been a significant effort to develop high specific impulse propellants for extending the range and payload capacity of upper stage ballistic missiles. A common problem encountered in these efforts centered upon the achievement and demonstration of an acceptable service life capability so to minimize forecast replacement requirements. Events showed that significantly higher performance generally produced a storage life penalty, even for controlled environment silo-stored missiles, that forfeited the potential economic gain, and even more severe limitations exist for projected future air borne systems.

A specific approach which was pursued vigorously was the attempted development and demonstration of an AlH_3/TVOPA propellant. These efforts received impetus once it was demonstrated that an internal gassing problem, associated with the use of aluminum hydride as a propellant fuel additive, could be overcome by incorporation of hydrogen gas scavengers. It, thereby, became the purpose of this program to provide an in-depth analysis of the aging life of a properly stabilized AlH_3/TVOPA propellant to determine this system's applicability in silo stored ballistic missiles.

More recently there was progress made in developing an alternative high performance propellant based upon the use of a fluorine binder polymer, PCDE. Range calculations showed that this latter system, which used aluminum instead of aluminum hydride as the solid fuel additive, would be superior to the AlH_3/TVOPA system in performance; moreover, the PCDE based propellants carried promise of better elevated temperature stability than the AlH_3/TVOPA systems to render the PCDE propellants potentially applicable in air-mobile ballistic missiles. As a result, program emphasis shifted toward these PCDE based propellants as representative samples became available for analysis under a propellant development and optimization contract conducted by Aerojet.

Consideration of air-mobility in future generations ballistic missiles stresses another facet of the problem. With silo stored missiles degradation in solid rocket motor performance results largely as a result of chemical aging processes operating within bond structures and propellant grains ultimately to the point where the motor can no longer be expected to function properly. With air mobile systems that may become subjected to temperature cycling, g-forces and vibration there is expected to result fatigue damage which even in the absence of chemical aging may produce failure.

Fatigue failure in propellants induced by the temperature cycling of motors has been the subject of numerous investigations, and though there

has been considerable progress in describing this failure mode mathematically, there persists the problem of forecasting the effects of chemical aging upon fatigue life. Therefore, efforts were to be made under this program to refine analysis and test methodology to allow service life forecasts to be made accounting for the combined effects of thermally induced chemical aging and strain induced fatigue.

1.2 OBJECTIVES

Propellants containing aluminum hydride as a fuel additive are prone to failure by internal gas generation causing the grains to develop voids or cracks. This problem can be alleviated or overcome by adding small quantities of a gas scavenger. With AlH_3/TVOPA propellants there is the additional problem of TVOPA thermal stability and compatibility with other ingredients, including the gas scavenger system. This program was to produce an unequivocal assessment of the aging life of AlH_3/TVOPA propellants to resolve the question whether this type of propellant can be used in silo stored ballistic missile motors.

Laboratory studies have shown that PCDE, an energetic fluorine binder prepolymer, if prepared in a suitably pure form is quite stable thermally, and that the material if properly formulated into a high solids propellant affords good propellant processibility, acceptable mechanical properties and high density specific impulse. Based upon these findings the Air Force contracted with the Shell Development Company to engage in the scale-up of this material, and with Aerojet General to develop, optimize and scale high performance PCDE propellants. Samples of the propellants developed by Aerojet were to be made available to this program for determining aging and fatigue life capability.

1.3 SCOPE

The aging life of a ballistically optimized and scavenger stabilized AlH_3/TVOPA propellant was to be determined by conducting a 12-month surveillance program at temperatures ranging from 20 to 50°C, and using elliptical tube surveillance specimens to simulate the gas diffusion path of larger grains. Analytical and mechanical tests were to be performed to quantify the aging process, and to allow the quick-time (test) data to be extrapolated to real-time (silo) storage conditions.

The predictive models to be used were those developed under a preceding contract. These models were to be refined to account for the fatigue effect associated with the long term storage of propellants under increasing internal gas pressure.

To assess the aging and fatigue life of PCDE propellants, the propellants were to be stored at temperatures ranging from 20 to 60°C for periodic chemical analysis, X-ray inspection and constant-load fatigue (creep-failure) testing. The test data were to be interpreted in terms of Weibull statistics leaning upon prior work done by Halpin at the Air Force Materials Laboratory in defining the service life capability of advanced structural composites in advanced aircraft application.

To implement and test the applicability of this approach with propellants, the initial testing was to be conducted with AlH_3/TVOPA and a model PCDE propellant. The test and analysis procedures were then to be used on ballistically optimized propellant samples to be supplied by Aerojet General.

(The reverse is blank)

2. SUMMARY

2.1 ALUMINUM HYDRIDE PROPELLANTS

An aluminum hydride propellant, that duplicated the Hercules VKW propellant except for addition of various gas scavengers, was processed into cylindrical and elliptical tube specimens for controlled environment storage at 20, 30, 40 and 50°C. The samples were monitored by periodic X-ray analysis to determine the onset of crack formation and samples of propellant cut from the center sections of the tubes were used to determine mechanical properties degradation as a function of aging time and temperature. Concurrently samples of the propellants with varying added gas scavengers were stored in sealed glass ampules for determining off-gas composition and generation rates.

The results of this investigation have been reported in detail in the technical reports issued under this contract; they can be summarized as follows:

(1) The estimated shelflife of a properly stabilized VKW-type aluminum hydride propellant is in excess of 3 years under 20°C storage, but decreases significantly at storage temperatures in excess of 20 to 30°C.

(2) The catalytic gas scavengers are effective in preventing hydrogen gas pressure build-up, and the scavenger activity is retained after 1½ years storage of the propellants at 20 to 30°C.

(3) With gas scavenger containing propellant failure, notably at elevated temperatures is caused by binder degradation to result in the generation of gases other than hydrogen accompanied by binder softening; the catalytic scavengers promote this degradation at temperatures in excess of 20 to 30°C.

(4) There is significant batch-to-batch variability even while carefully controlling material, formulation and processing variables. This is attributed to differences in the degree of particle surface attrition during mixing, and it poses a very difficult problem in propellant quality control.

It is the last mentioned problem that would cause prohibitive problems in motor manufacture. Even though careful adjustment of the formulation, notably with regard to curative system and gas scavengers, may be expected to afford 20 to 30°C age lifes in excess of 5 years, there would presently

not exist the analytical means for controlling critical material and processing variables to assure motor-to-motor equivalence in age life capability. Analytical data, identifying an inadequate propellant batch, would not become available until months after the facts. Recognition of this problem, and failure of range calculations to evidence more significant potential gains, caused further work with this propellant to be curtailed.

2.2 PCDE PROPELLANTS

The program evaluated two PCDE propellants, namely a model PCDE propellant processed at LPC using di-n-butylphthalate as a chemically inert plasticizer, and a ballistically optimized PCDE propellant processed at Aerojet using a nitrate ester plasticizer. The two propellants differed further in the source of the PCDE prepolymer. The propellant processed at LPC used PCDE prepared by the Shell Development Company, while the Aerojet propellant was processed with PCDE manufactured by Hercules Inc.

2.2.1 Model PCDE Propellant

This propellant was processed in a 1-gallon Baker Perkin mixer and vacuum cast into elliptical tubes of varying length for storage at 40 and 60°C. The specimens were monitored by periodic X-ray analysis, and aging induced changes in mechanical properties were determined using uniaxial tensile and constant-load creep failure tests. Gassing rates and off-gas compositions were determined using both neat PCDE polymer and propellant stored in sealed glass ampules. The results can be summarized as follows:

(a) The X-ray analyses showed no gross failures after 180 days storage at 40 and 60°C, nor was there any noticeable deformation of the elliptical tubes to suggest internal gas pressure.

(b) Off-gas evolution, though noticeable initially, decreased markedly with storage time to suggest a residual impurity as the gas source.

(c) The uniaxial and the constant-load creep failure tests show a distinct reversal in trend, an initial 100-120 day period wherein the propellant undergoes softening being followed by renewed hardening. The data are indicative of a secondary cure process that may be peculiar to the PCDE polymer structure.

2.2.2 Ballistically Optimized PCDE Propellant

This propellant was received from Aerojet in the form of blocks and elliptical surveillance specimens. These were stored at 30, 40 and 50°C, and monitored using the same techniques as described for the model propellant. The results showed significant differences between these two propellants:

(a) Monitoring the elliptical tube specimens by periodic X-ray analysis showed gross failure by cracking within relatively short storage periods even at 30°C.

(b) Off-gas generation rates were comparable to the rates observed with the model propellant relying upon Arrhenius extrapolations for comparing the two sets of data. This implies that the early failures were not caused by a severe incompatibility problem.

(c) In contrast with the model PCDE propellant, there was a significant difference between the uniaxial tensile and the constant-load creep failure test data. Storing the propellant at 30 and 40°C had no significant effect upon uniaxial tensile properties, while the constant-load creep failure tests showed distinct softening at 30°C, and softening with a reversal to renewed hardening at 40°C.

The observation that aging at 30 and 40°C caused the constant-load creep-failure data to change significantly while the constant strain rate tensile data remained unchanged leads one to believe that this propellant had undergone limited crosslinking only; this could cause it to fail by plastic flow even under low internal gas pressure.

Since different lots of PCDE were used in processing the two propellants, it cannot be stated if any deficiency in cure may be attributable to either a formulation, processing or prepolymer deficiency[1]. Whatever the reason, the results obtained with the ballistically optimized propellant are not necessarily to be considered indicative of the potential of PCDE as propellant binder polymer.

2.2.3 PCDE Propellants, General

Considering both sets of data one can state the following conclusions:

(a) The PCDE polymer appears to have good thermal stability, but as presently produced contains a structural impurity that decomposes, even at 30°C, with formation of gas. Preconditioning the polymer at 50 to 60°C might neutralize this impurity.

---

[1] Upon processing nitrate ester plasticed PCDE propellants under an earlier program LPC also experienced difficulties in attaining a satisfactory degree of cure.

(b) The cured polymer undergoes network degradation during initial storage at 30 to 60°C as evidenced by softening of the propellants. This degradation occurs concurrently with the gas evolution, and the same structural impurity might be responsible for both effects.

(c) After an initial storage at temperatures in excess of 30°C a secondary cure or crosslink process enters into play to reverse the softening process, and to cause hardening of the propellant. This process does not seem to represent a normal post-cure reaction involving the curative; instead, it may reflect a pecularity of the basic structure of this polymer. Longer surveillance periods are needed, however, to determine whether this hardening process plateaus, or whether it continues to pose a significant problem.

2.3 TEST METHODS DEVELOPMENT

It was the further purpose of this program to implement and test two statistical cumulative damage analysis approaches for the purpose of defining the effects of chemical aging upon the distribution of failures under given temperature and load conditions. These two approaches were Halpin's Statistical Cumulative Damage approach as applied to the analysis and interpretation of constant-load creep failure test data, and Kaelble's analysis of constant strain rate tensile data.

2.3.1 Halpin's Statistical Cumulative Damage Approach

Halpin showed that the constant-load creep failure characteristics of rubbers or structural composites can be defined by a two parameter Weibull survival probability function. Data produced under this program, and under parallel programs applying this concept with conventional CTPB and HTPB propellants, showed that chemical aging produces a non-linear damage effect. To define this effect it is necessary to use an expanded Weibull expression, and the report elaborates upon this modification for analyzing and interpreting constant-load creep failure data with AlH_3 and PCDE propellants undergoing thermal aging.

2.3.2 Kaelble's Kinetic Analysis of Constant Strain Rate Tensile Data

Kaelble, working with Kraton triblock copolymers, showed that the constant-load survival probability function can be derived from constant strain rate tensile data. This program tested this approach with AlH_3 and PCDE propellants, and it was found that Kaelble's analysis of the constant strain rate tensile data provides a valuable diagnostic tool for interpreting

propellant mechanical properties in terms of the governing physico-chemical properties of the binder, and that it provides an expedient for determining the parameters of the load-time and temperature-time shift factors. Further methods development appears necessary, however, to enable this approach to be relied upon for predicting the effects of chemical aging upon constant-load creep failure distributions. In its present state of development, Kaelble's kinetic analysis of constant strain rate tensile data complements, but does not substitute for the Halpin approach.

(The reverse is blank)

3. TECHNICAL EFFORT

3.1 PROCEDURES

3.1.1 Propellant Processing

Propellants were prepared as part of this program in either a 150 cc conical ARC or a 1-gallon Baker Perkins mixer, both equipped for bottom discharge and operated under -30°F dew point atmospheric environment. Where multiple mixes were needed for preparing the necessary number of test specimens, considerable care was taken to duplicate processing and cure cycles.

3.1.2 Propellant Surveillance

The propellants studied under this program tend to undergo thermal degradation accompanied by gas evolution. This may cause internal pressurization and failure by gas void or crack formation. The rate of pressurization is dependent upon gas generation and diffusion rates, the latter being dependent upon specimen size and geometry. As a result, a small test specimen may equilibrate at a relatively low internal gas pressure while a large grain would suffer a significantly higher internal pressure build-up to fail within a correspondingly shorter time period. A realistic surveillance program would therefore necessitate relatively large test specimens with associated large propellant quantity requirements. To circumvent this problem the program relied upon the use of elliptical tube specimens, a method introduced by Rohm and Haas (Ref 3-1) as a means of simulating large diffusional paths with small laboratory test specimens.

For surveillance purposes the specimens were packaged in polyethylene bags under very low humidity environment and stored at the appropriate temperatures. Internal gas pressure build-up was detected by a change in circumference of the elliptical tubes, while periodic inspection by X-ray was used to determine the onset of void or crack formation. For determining changes in the mechanical properties propellant was cut from the center sections of the tubes. A more limited number of cylindrical blocks of varying dimensions were carried through surveillance and tested in parallel for verification.

For determining gas generation rates and off-gas compositions, 1- to 5-gram quantities of the propellants were sealed into glass ampules using argon as the fill gas.

The conditioning chambers generally were controlled within ±1°C and monitored remotely to guard against temperature excursions.

3.1.3 Off-Gas Analyses

For determining gas generation rates and off-gas composition ampules were periodically withdrawn from surveillance and crushed in a volume calibrated gas sampler. Measured volumes of the gas were then analyzed by gas chromatography or mass spectrometry. This procedure afforded high accuracy for the non-condensible gases (N_2, CO_2, CO, H_2, N_2O, C_xH_y) but qualitative data only for the more readily condensible species (HCN, HF, H_2O).

For shorter term gas evolution measurements mercury-type manometers were used.

3.1.4 Mechanical Properties Testing

Uniaxial Tensile Testing. Propellant cut from the center sections of the elliptical tubes was microtomed to prepare mini-thin tensile specimens which were end-bonded to wooden tabs. The testing was done over a broad range of temperatures and strain rates to provide the data basis for the kinetic analysis, to be discussed in Subsection 3.1.5, and to be elaborated on further in Appendix A.

Creep-Failure Testing. The creep-failure (constant-load fatigue) test was used for determining the distribution of failures under given temperature and load conditions. For this purpose the mini-thin tensile specimens, in groups of 20 to 40, were mounted on a rack inside a dry box and loaded to the appropriate weight level. An optical system was used to monitor and record the failure events. Halpin's statistical cumulative damage approach (Ref 3-2) was used to analyze and interpret the results, this approach is outlined below and is further elaborated upon in Appendix A.

3.1.5 Statistical Analyses

Two procedures were used for the statistical analysis of the data and for providing an assessment of service life capability in terms of predicted failure distributions; namely Halpin's treatment of creep test data and Kaelble's treatment of constant strain rate tensile test data. These two data treatments are complimentary.

Halpin's Analysis of Creep-Test Data. Halpin showed that the distribution of failures of elastomers or structural composites under constant-load-to-failure conditions can be defined by a Weibul survival probability function (Equation 1)

$$N(t)/N_o = \exp - (kt)^n \qquad (1)$$

where N(t) is the number fraction of the total number (N_o) of test specimens remaining intact at time t, k a scale parameter, and n a shape parameter. Equation 1 can be rearranged to Equation 2,

$$\log\left(-\log\left(N(t)/N_o\right)\right) = n \log t + n \log k - 0.362 \qquad (2)$$

and plotting the data in accordance with this equation enables one to determine the numerical values for k (scale parameter) and n (shape parameter) by determining slope and intersect (Figure 3-1).

Equation 1 is based upon the concept that all elastomers or composites contain an infinite number of microscopic or sub-microscopic flaws that upon subjecting the sample to stress will grow, first at a relatively constant linear rate until some flaws reach critical dimensions; at this point the growth rate increases exponentially to produce failure. Equation 1 thereby states the probability of any one of this large number of flaws to reach critical dimensions at a given linear flaw growth rate, k. The shape parameter, n, reflects the dimensionality of the internal stress field and flaw size distribution.

In order for a flaw to propagate in a viscoelastic medium, polymer chains must be disentangled and crosslinks must be broken. As a result, k constitutes a polymer network property that is temperature, stress and stress rate sensitive, and Halpin showed that this sensitivity can be accounted for by introducing the appropriate shift factors. This results in Equation 3

$$k = \frac{k_o}{a_T \cdot a_\sigma \cdot a_C} \qquad (3)$$

where a_T is the Williams-Landel-Ferry temperature-time shift factor, a_σ is the Halpin-Bueche stress-time shift factor based on Ferry's power law, and a_C is a chemical shift factor to account for variations in effective crosslinks. Halpin showed that using these shift factors the failure distribution curves obtained under varying temperatures and loads can be shifted and superimposed. This, in turn, provides the means for data extrapolation from laboratory test to real life conditions, however, ignoring chemical aging effects.

This program was to test the applicability of this statistical approach to propellants under aging with the following general results:

(1) Equations 1 and 3 were found to satisfactorily describe the distribution of failures for some of the propellants that were tested. Notably with aged propellants, however, the distribution was multi-modal, and to account for this Equation 1 had to be expanded into Equation 4:

$$N(t)/N_o = \alpha_1 \exp -(k_1 t)^{n_1} + \alpha_2 \exp -(k_2 t)^{n_2} + \alpha_3 \exp -(k_3 t)^{n_3} \qquad (4)$$

where the subscripts denote the individual sub-populations, and α_i the number distribution of test samples among the

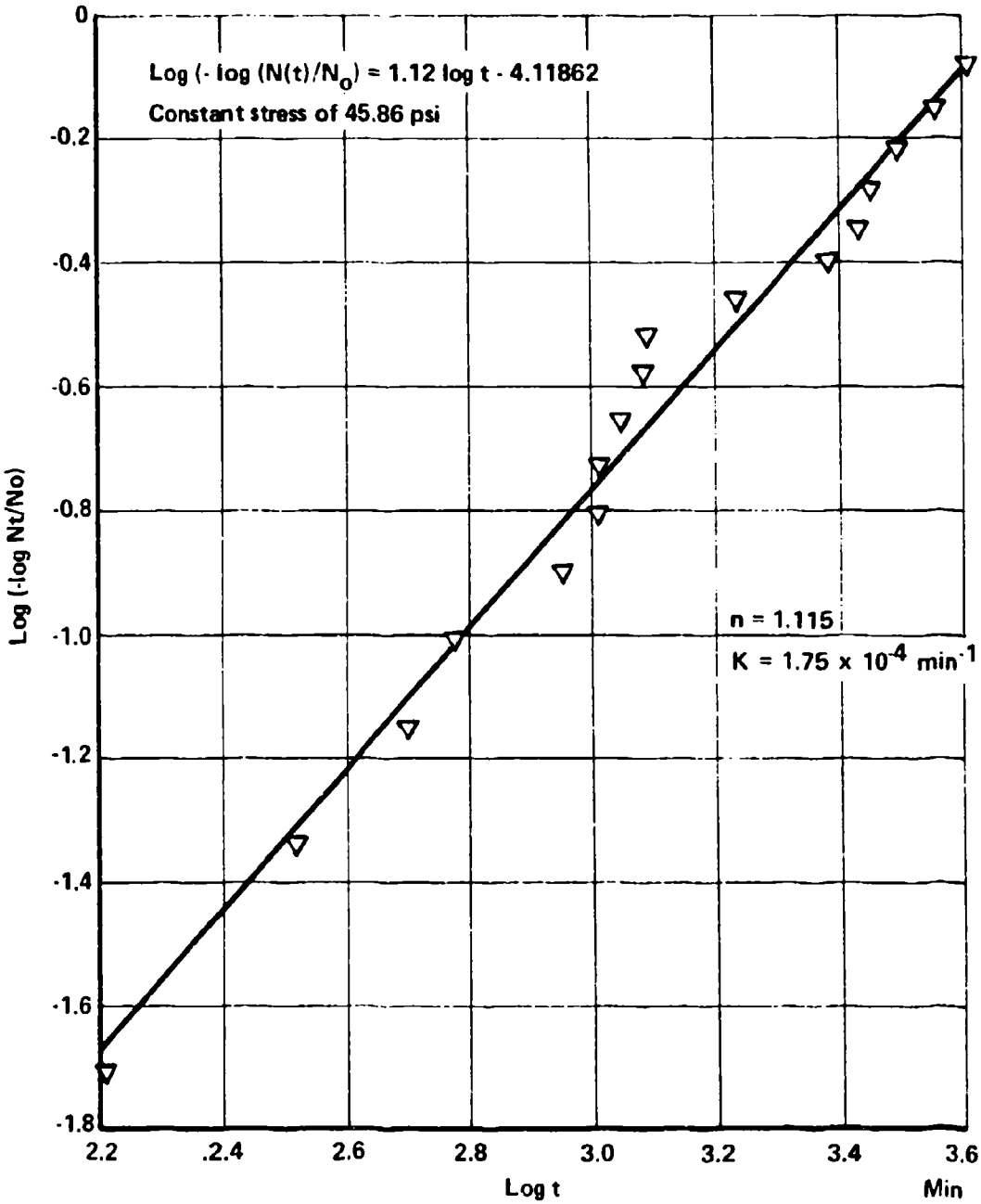

Figure 3-1 Weibull Plot, Creep-Failure Distribution AlH_3/TVOPA Propellant (46 psia)

sub-populations. Computerized curve-fitting was used to determine the individual values for α_i, k_i and n_i, and it was generally found that the parameter varying among the sub-populations was n rather than k.

(2) Some of the propellants were creep-failure tested at several loads and temperatures, and it was shown that the failure distribution curves could be shifted to afford a reasonably good data superposition (Figure 3-2). There were difficulties, however, in determining the stress-time shift factor with sufficient accuracy to enable reliable long-term forecasts to be made.

The Halpin-Bueche stress-time shift factor (Equation 5) requires knowledge of the long-term stress value, $\sigma_{(\infty)}$, which is the limiting stress below which failure will not occur and of the exponent, $1/\overline{n}$. Creep failure tests with propellants are highly stress-level

$$a_\sigma = \frac{t_b}{t_b'} = \left(\frac{\sigma_b(t') - \sigma_b(\infty)}{\sigma_b(t) - \sigma_b(\infty)} \right)^{1/\overline{n}} \qquad (5)$$

sensitive, and exceeding a relatively narrow practical range results in undesirably short average failure times, or in unduly long exposure of the test specimens to atmospheric environment. Alternatively, the information necessary for deriving the stress-time shift factor can be obtained by the kinetic analysis of the constant strain-rate tensile test data; this procedure requires various corrections to be made, and it is not fully satisfactory either.

Chemical aging generally was found to cause both k and n to increase, and there is indication that it also causes the value for $\sigma_{(\infty)}$ to change. This renders the prediction of the effects of chemical aging upon projected real-life failure distribution a more difficult task than was suggested by Halpin, and related matters will be discussed in more detail in later sections.

(3) Another difficulty arose in selecting the reference conditions for normalizing the scale parameter in accordance with Equation 3. Largely because of differences in the long-term stress values ($\sigma_{(\infty)}$) it may not be practical to test different propellants at the same stress level, and the selection of some arbitrarily chosen reference conditions becomes necessary. There was some incentive to define k_o as the rate that would cause 50 percent of the specimens to fail within a unit of time. The values for k_o meeting this requirement can be calculated by substituting $\log(-\log 0.5) = -0.521$, and $n \log t = 0.0$ into Equation 2 to yield

$$\log k = -\frac{0.159}{n}$$

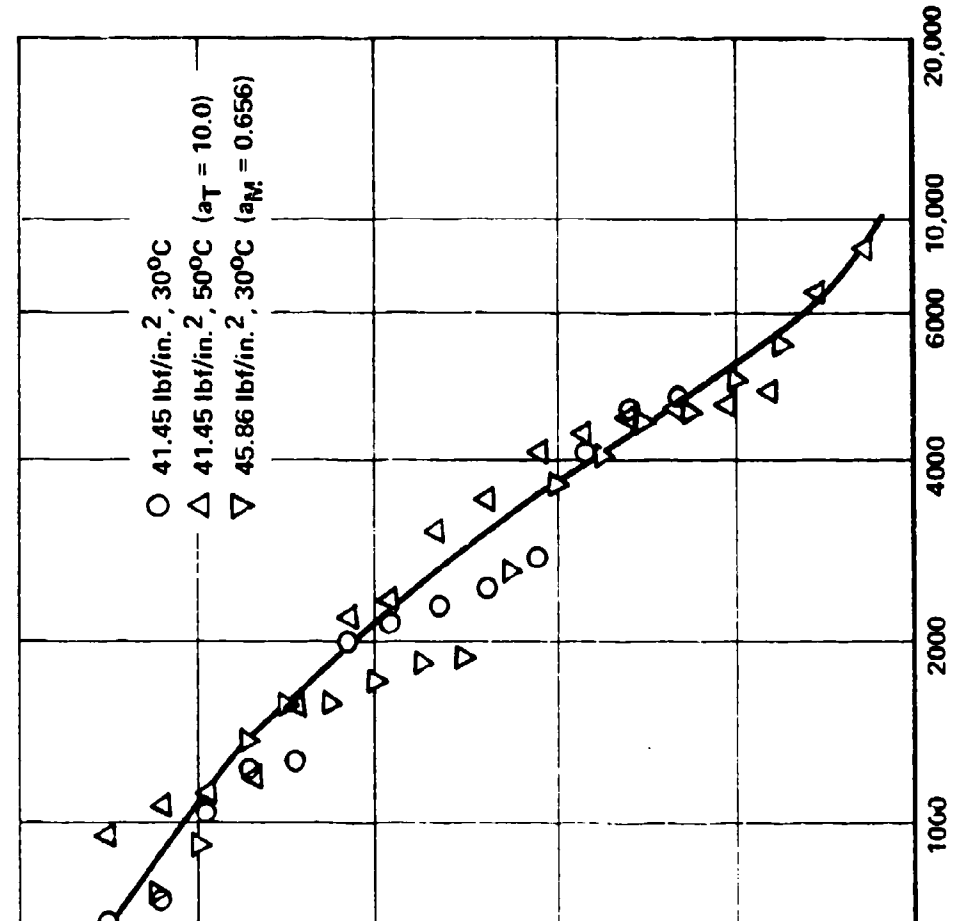

Figure 3-2 Superposition of Creep-Failure Distributions Using the Temperature-Time and the Stress-Time Shift Factors - AlH_3/TVOPA Propellant

In other words, k under these conditions is dependent only upon n, the propellant-to-propellant differences now residing with $\sigma_{(\infty)}$ and $\sigma_b(1.0)$, the latter being the load required to cause 50 percent of the specimens to fail within a unit of time at a given temperature. This reduces the expression for the stress-time shift factor (Equation 5) to Equation 6

$$a_\sigma = \frac{t_b}{1} = \text{constant} \left(\sigma_b(t) - \sigma_b(\infty)\right)^\eta \qquad (6)$$

It implies that the constant-load fatigue behavior of a propellant can be characterized by defining the values of n, $\sigma_{(\infty)}$, $\sigma_{(1)}$, η and the values needed for deriving the temperature-time shift factor. Experience further shows that η may be a constant, all propellants tested seemed to have η-values ranging around 2.67.

Normalizing the k-values to $t_b^{50\%} = 1.0$ using the stress-time shift factor, and comparing the thus derived value with the theoretical value ($\log k_o = -0.159/n$) provides a test of the accuracy of the data extrapolation.

Kinetic Analysis of Constant Strain Rate Tensile Test Data. While studying the mechanical properties of Kraton triblock copolymers, Kaelble (Ref 3-3) showed that the information necessary for defining failure distributions under constant load can be derived from constant strain rate uniaxial tensile data. This provides an expedient for producing information, for example, to derive the temperature-time and stress-time shift factors, that otherwise would require excessive test time requirements. In addition, Kaelble's kinetic analysis of the constant strain rate tensile data affords a more detailed description of the failure process to aid in the interpretation of mechanical test data in terms of the controlling physico-chemical parameters. For these reasons this approach was implemented under this program in parallel with the Halpin approach.

The following outlines Kaelble's approach, and modifications introduced while implementing this approach with propellants:

The stress response of an ideal rubber is described by Equation 7 where

$$\sigma = \epsilon \frac{E_m(t)}{1 - \lambda^2/\lambda_m^2} \qquad (7)$$

$E_m(t)$ is the time dependent network modulus, and λ_m the ultimate extensibility ($\lambda = \epsilon + 1$), the latter being a function of the number average bonds between effective crosslinks.

If an elastomer sustains damage as it is being strained, the stress response falls below the values predicted by Equation 7, and Kaelble introduced a damage function, $B(\epsilon, t)$ to account for this deviation (Figure 3-3).

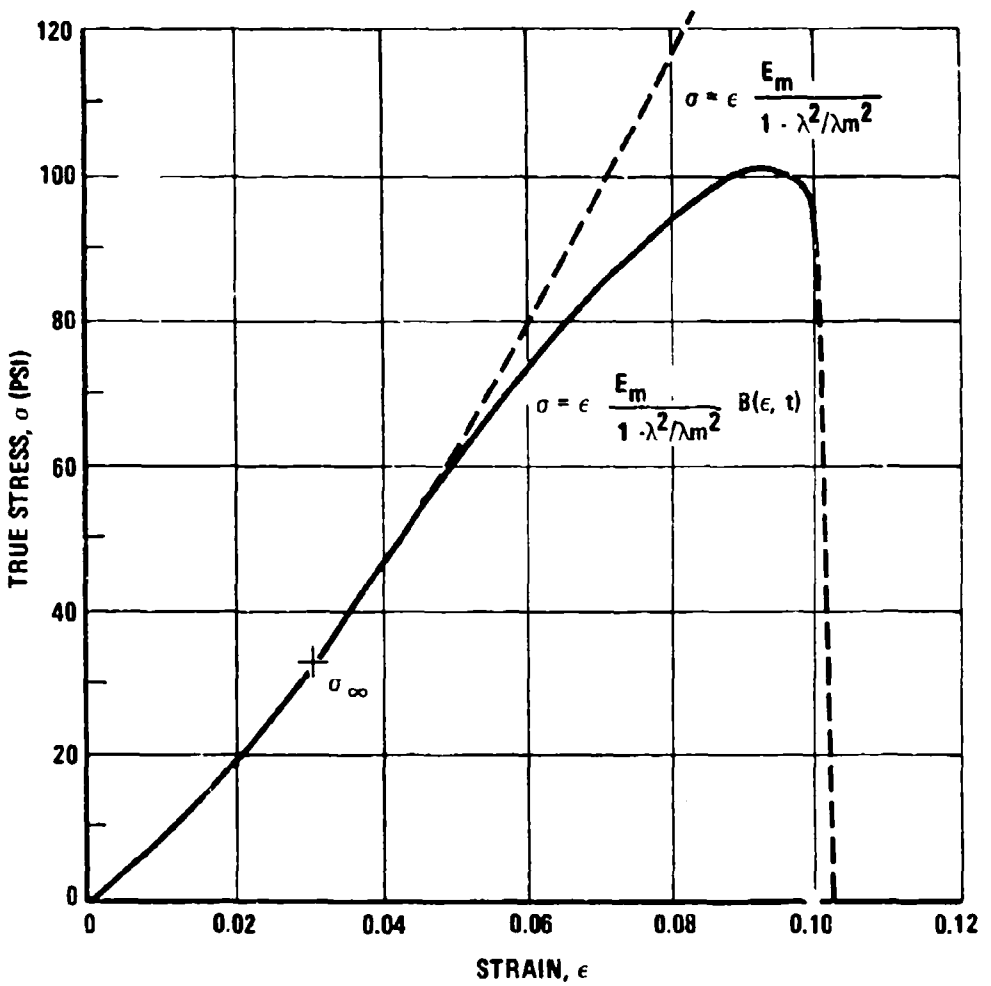

Figure 3-3 Kaelble's Damage Function Elastomers

This results in Equation 8 that describes the experimentally recorded stress-strain curve:

$$\sigma = \epsilon \frac{E_m(t)}{1 - \lambda^2/\lambda_m^2} B(\epsilon, t) \quad (8)$$

The damage function, $B(\epsilon, t)$, which can be derived by computer analysis of a λ^2 versus ϵ/σ plot of the test data can be equated to the Halpin survival probability function (Equation 1) by introducing an appropriate strain rate shift factor (Equation 4).

$$B(\epsilon, t) = \exp - \left(\frac{kt}{a_{\dot{\epsilon}}}\right)^n \quad (9)$$

Upon applying this analysis method to propellant constant-strain rate tensile test data one commonly observes a two-step failure process characterized by two damage functions (Figure 3-4). The first damage function, B_1, describes the initial stress relaxation process attributable to cavitation. With propellants this process starts at very low strain levels implying irreversible damage to occur almost immediately upon straining. The second process, described by the damage function B_2, reflects the flaw or crack growth process that ultimately lead to failure, and it is found that the constant-load creep failure distribution can be defined by substituting the values for B_2 into Equation 9.

Critical to this analysis is the definition of the point on the λ^2 versus ϵ/σ data plots that signifies the onset of the flaw growth or tear process. This point represents the critical stress, σ_{cr}, with $B_1 = 0$ and $B_2 = 1.0$ unless there is overlap between the two failure processes. The critical stress decreases with decreasing strain rate, and graphic extrapolation of σ_{cr} values determined over a wide range of temperatures and strain rates enables the asymptotic value to be determined; this value represents the long-term stress, $\sigma_{(\infty)}$ which appears in Equation 5 defining the stress-time shift factor.

The general experience in applying this analysis technique with propellants can be summarized as follows:

(1) With unaged propellants the failure initiating cavitation step generally is clearly discernible. However, there can be some overlap between this step and the subsequent flaw growth step to prompt difficulties in defining the correct values for σ_{cr}. This translates into errors in determining $\sigma_{(\infty)}$ and the Halpin scale parameter k.

(2) With the aged propellants the cavitation step may no longer be observed implying that chemical aging caused degradation of the binder-filler bond to eliminate the reenforcing action of the filler. This is commonly paralleled by an increase in the values of n in the Halpin constant-load distribution function.

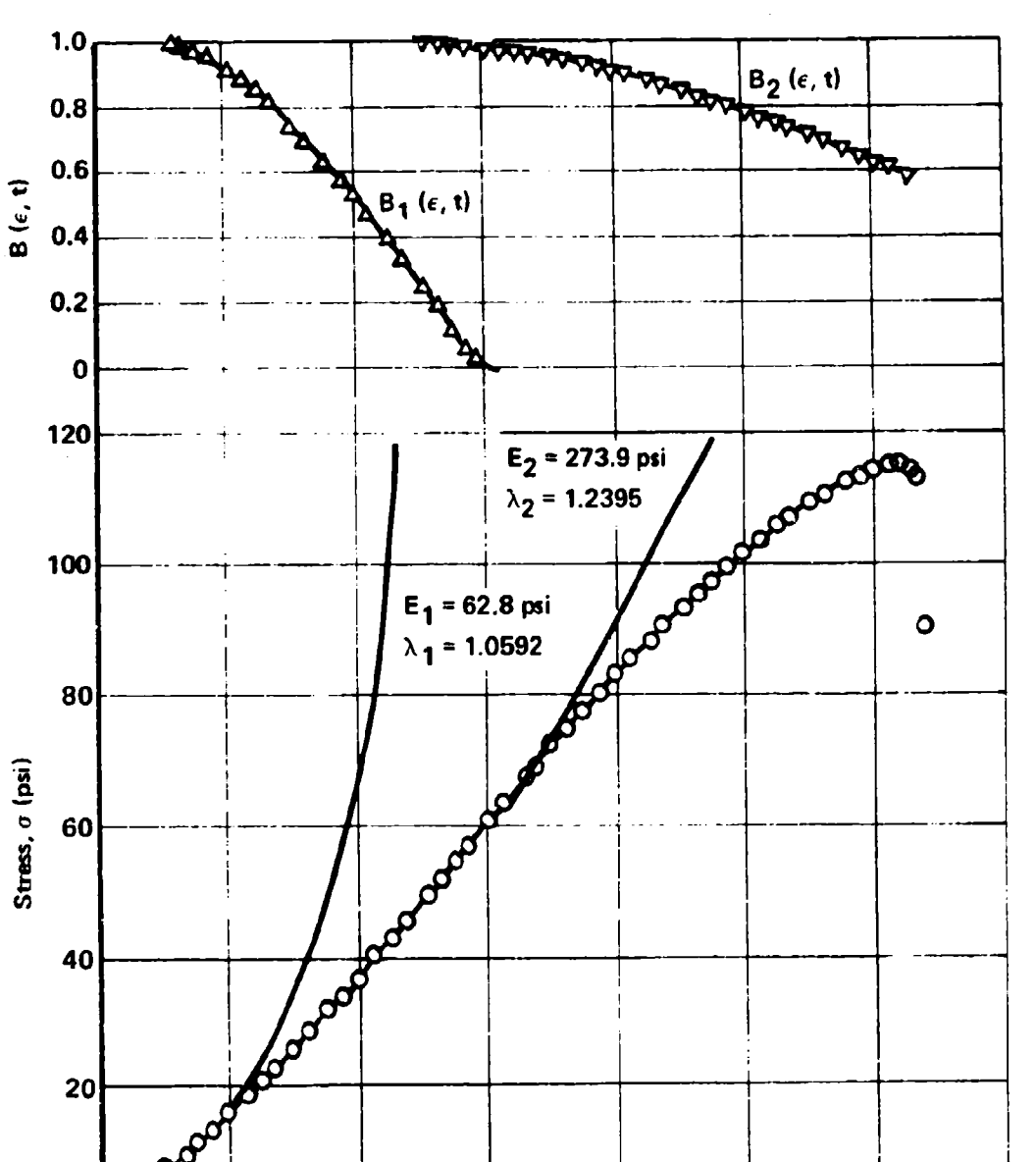

Figure 3-4 Cumulative Damage Functions: $B_1(\epsilon, t)$ for Cavitation and $B_2(\epsilon, t)$ For Crack Growth. AlH_3/TVOPA Propellant at 30^0C and Strain Rate of 1.108 in./in.-min.

(3) By its ability to differentiate between the two failure processes, the kinetic analysis of constant strain rate tensile data rationalizes the dependency of propellant mechanical properties upon controlling compositional and structural features. Specifically, it enables differentiation between properties and aging effects attributable to binder-filler interaction as opposed to properties and aging effects more intimately associated with polymer network structure and degradation.

3.2 RESULTS

3.2.1 Aluminum Hydride/TVOPA Propellants

Aluminum hydride upon storage undergoes slow degradation with generation of hydrogen gas. Though decomposition rates at 20°C are minor, they are nevertheless sufficient to cause a gas cracking problem if the material is used as a solid propellant fuel additive. Hydrogen gas generation also occurs as a result of interaction with moisture and reactive propellant ingredients notably during mixing where surface shear abrasion counteracts surface passivation.

The problem was analyzed in-depth under Contract F04611-69-C-0038, and it was found that even allowing for further improvements in material stability propellants with a minimum 5 years 20°C aging life could not be produced unless means were found to scavenge the small, but significant quantity of hydrogen gas being generated within the grains. This led to the evaluation and demonstration of a catalytic principle that consumed the internally generated gas by a hydrogenation process.

In a model propellant, using a di-n-butyl phthalate plasticized polyester binder, this catalytic scavenger totally suppressed internal hydrogen gas pressure build-up even upon prolonged storage at elevated temperature. This program was to apply this principle with a ballistically optimized AlH_3/TVOPA propellant, and it was to demonstrate that such a propellant, if properly stabilized, would have a 20°C aging life in excess of 5 years. This was to be accomplished by conducting a 1-year surveillance program and providing the analytical data needed for the time-extrapolation of the data.

The results of this investigation have been summarized in detail in technical interims reports issued under this contract (Ref 3-4), and except for a brief summary of the surveillance and analytical test data this report will elaborate only upon a matter of more general interest, namely the fatigue effect associated with propellant internal gas pressurization.

The models that were established and used under the preceding programs to predict the rate of internal gas pressurization as a function of gas generation

rates, gas solubility and gas diffusion rates to determine the point in time where the internal gas pressure would exceed the system's stress capability did not account for the associated fatigue effect. Moreover, they afforded only mean failure times which is of limited practical interest. Therefore, to account for the fatigue effects and to produce a more detailed forecast of failure distributions this program implemented the Halpin fatigue life analysis approach.

Propellant Surveillance. Propellant duplicating the Hercules VKW formulation except for the addition of gas scavengers and variations thereof was loaded into elliptical tube specimens of varying length for simulating different size grains with respect to gaseous diffusion paths.

The tubes were stored at 20, 30, 40, and 50°C under dry nitrogen and inspected periodically for changes in dimensions (circumference) and crack development (X-ray). At intervals tubes were withdrawn and cut to prepare mini-thin tensile specimens.

The results of the surveillance are summarized in Table 3-1. The data show:

- The catalytic scavengers are effective in retarding internal gas pressure build-up over prolonged time periods; some of the 30 to 40 cm tubes loaded with stabilized propellant remaining intact after 574 days storage at 30°C.
- The critical length is 6 to 12 cm at 40°C and 12 to 18 cm at 30°C.
- There is significant data scatter attributable to both AlH_3 lot-to-lot and propellant batch-to-batch variations.
- The cylinders that were placed into storage at 40°C to verify the elliptical tube failure time data[1] revealed that failure upon prolonged storage at moderate temperature occurs as a result of binder softening. This was confirmed by testing propellant cut from the tubes. The data showed little mechanical properties degradation to occur until cracks become noticeable on X-ray; at this point there was marked softening attributable to hydrolytic cure linkage degradation.
- At 20°C none of the samples failed within 594 days, and Arrhenius type extrapolation of the 20 to 50°C data indicates an average 20°C aging life in excess of 1000 days.

Off-Gas Analyses. To determine the production rates and the composition of the off-gases, propellant representative of the various mixes was

---

[1] A critical factor in using elliptical tubes for propellant surveillance purposes involves the maintenance of a bond between propellant and tube wall. Debonding, opening a gas path, drastically shortens the diffusional path to afford grossly erroneous data.

Table 3-1

PHASE I: SURVEILLANCE DATA SUMMARY

	Mix Number/Days to Failure/Failure Mode										
	Tube Length, cm									Cylinder Diameter, cm	
	6	12	18	24	30	40	50	60	80	12	17
68°F											
Control						X/>574/--	X/>574/--	X/>574/--	X/>574/--		
						A/>431/--	A/>431/--	A/>431/--	A/>431/--		
						B/>431/--	B/>431/--	B/>431/--	B/>431/--		
Scavenger A						F/>574/--	F/>574/--	F/>574/--	ZZ/>574/--		
						G/>574/--	G/>574/--	G/>574/--	ZZ/>574/--		
Scavenger B						K/>594/--	K/>594/--	K/>594/--	K/>594/--		
						L/>594/--	L/>594/--	L/>594/--	L/>594/--		
Scavenger C						R/>594/--	R/>594/--	R/>594/--	R/>594/--		
						S/>594/--	S/>594/--	S/>594/--	S/>594/--		
86°F											
Control			X/>574/--	X/ 350/C	X/>574/--	X/ 203/C					
			A/>431/--	A/>431/--	A/>431/--	A/>341/--					
			B/>431/--	B/>431/--	B/>431/--	B/ 59/C					
Scavenger A			F/>574/--	F/>574/--	H/>574/--	F/>574/--					
			F/>574/--	G/>574/--	H/>574/--	G/>574/--					
Scavenger B			K/ 532/aC	K/ 494/aC	M/ 464/aC	K/ 464/aC					
			L/ 494/aC	L/ 494/aC	M/ 464/aC	L/ 464/aC					
Scavenger C			R/ 494/aC	R/ 494/aC	R/ 464/aC	R/ 464/aC					
			S/ 494/aC	S/ 494/aC	S/ 464/aC	S/ 464/aC					
104°F											
Control		AA/345/C	AA/ 309/C	W/ 59/C[a]	W/ 59/C[a]					C/ 294/C	D. F./294/C
		AA/365/C	X/ 147/C	W/ 59/C[a]	W/ 59/C[a]						
			A/ 37/C	A/ 37/C	X/ 54/C[a]						
			B/ 147/C	B/ 37/C	A/ 37/C						
					B/ 147/C					H/ 266/F	I. J/238-252/F
Scavenger A		F/224/F	F/ 210/V	F/ 210/V	H/ 210/V						
		G/224/F	G/ 210/V	G/ 210/V	H/ 210/V					M/>453/--	N. P/287/Soft
Scavenger B		L/182/F	K/ 140/V	K/ 140/V	M/ 140/aC, V						
		N/182/F	L/ 140/V	L/ 140/V	M/ 140/aC, V					T/ 287/Soft	U. V/224/F/Soft
Scavenger C		U/182/F	R/ 140/V	R/ 140/V	T/ 140/aC, V						
		V/182/F	R/ 140/V	S/ 182/V	T/ 140/aC, V						
122°F											
Control	AA/205/F (1)	AA/142/aC	AA/ 128/F	X/ 12/C[a]							
		AA/142/aC	AA/ 128/F	X/ 19/C[a]							
				A/ 9/aC							
				B/ 9/aC							
Scavenger A	J/119/C	H/ 99/V	F/ 99/C	F/ 99/C							
	J/119/C	H/ 99/V	G/ 99/V	G/ 99/V							
Scavenger B	P/112/F	N/ 59/F	K/ 59/F	K/ 59/F							
	P/112/F	P/ 59/F	L/ 59/F	L/ 59/F							
Scavenger C	U/112/F	V/ 59/F	R/ 59/F	R/ 59/F							
	V/112/F	U/ 59/F	S/ 73/F	S/ 59/F							

[a] Prepared with incompatible lot of AlH_3 (Lot No. B 11).

NOTES: S = swell, C = crack, V = void, F = fissures, aC = small crack.

(1) AA = specimen, 6 cm, at 122°F was sacrificed after 142 days to determine propellant condition.

sealed into glass ampules for storage at 20, 30, 40 and 50°C and periodic gas chromatographic analysis. The gas species that were determined were H_2, CO_2, CO, N_2, NO, N_2O and hydrocarbons (C_2H_6, C_2H_4); the more highly soluble species (H_2O, HF, HCN) known to be formed but requiring more complex analysis techniques were not determined routinely. The results were as follows:

- The gaseous products produced in largest quantity are hydrogen and CO_2; the other products, formed in lesser quantities, are CO, N_2, N_2O and NO together with traces of hydrocarbons.

- Hydrogen Gas is generated in significant amounts by the control propellants (no added scavenger) with significant batch-to-batch variations notably during the initial storage period. Typical values after 160 days storage are:

  2.3 to 3.7 micromoles/gram at 20°C

  11 micromoles/gram at 30°C

  13.7 to 16 micromoles/gram at 40°C

  28 to 30 micromoles/gram at 50°C

  The addition of catalytic scavenger totally suppresses hydrogen gas evolution at 20 and 30°C, even after 400 days storage, with small quantities of H_2 appearing at 40°C after approximately 100 days implying gas generation rates in excess of scavenger rate capacity. Hydrogenation tests confirmed that even after prolonged propellant storage the catalyst remains active.

- Carbon Dioxide. Next to hydrogen the most significant gas species is CO_2. Typical values after 160 days storage are:

  3 to 5 micromoles/gram at 20°C

  2.5 micromoles/gram at 30°C

  2 micromoles/gram at 40°C

  8.3 to 13.3 micromoles/gram at 50°C

  Most of this gas, however, is generated during the initial 100 days storage period contrasting hydrogen gas evolution which increases with time. Scavenger addition enhances CO_2 generation at the higher temperatures.

- Upon comparing the times to failure of the elliptical tube specimens with the gas generation data, failure was shown to occur after 4 to 7 micromoles CO_2/gram propellant has been generated.

The data show that over a 300 to 400 day observation period the catalytic gas scavengers are effective in preventing internal gas pressure build-up due to hydrogen gas generation; however, the data also evidence significant batch-to-batch variations in internal gas pressures due to other gases. As a

result there would be significant grain-to-grain differences in internal gas pressure to cause significant data scatter in failure distributions.

Constant-Load Fatigue Behavior. Mini-thin tensile specimens, in groups of 20, were cut from the elliptical tubes to determine failure distributions under constant load and as a function of aging time at the various temperatures. Because of the small dimensions of the test specimens, any internal gas pressure is lost during sample preparation, and the observed failure distribution is strictly a function of the applied load. These tests, however, provide the information that is needed to determine, in conjunction with gassing rate data, the effects of internal gas pressurization upon failure distributions.

(1) Unaged Propellant. Propellant stored under dry nitrogen in a conditioning box if subjected to loads ranging from 41 to 46 psia (temperature 20 to 50°C) affords a unimodal distribution of failures if the data are plotted in accordance with Equation 2.

A typical data plot is shown in Figure 3-5. Typical values for n and k as a function of applied load and temperature for unaged (cold stored) AlH_3/TVOPA propellant are quoted in Table 3-2 and may be commented upon as follows:

- Increasing the test temperature from 30 to 50°C has no effect upon the shape parameter, n. It implies that the data can be superimposed using the WLF temperature-time shift factor, a_T. Numerical values for a_T, derived from the constant strain rate tensile tests are quoted in Table 3-3.

- Upon increasing the load from 41 to 46 psia the shape parameter, n, decreases from 1.4 to 1.2, which is considered to be within experimental error. It implies that the data can be shifted using the stress-time shift factor (Equation 5), and both the constant load creep failure data and the Kaelble treatment of the constant strain rate tensile data were used to determine the parameters for this shift factor. The two sets of data are summarized in Table 3-3. They reveal a discrepancy in the values for $\sigma_{(\infty)} \frac{286}{T}$ and $\sigma_{(1)} \frac{286}{T}$ which may be attributed to difficulties in determining σ_{cr} using the stress-strain and derivation data plots. Judging from test data with other propellants, the exponent $1/\bar{n}$ (Equation 5) appears to assume a constant value around 2.67.

- Table 3-3 also provides a comparison of the k_o values derived by extrapolation of the constant-load and constant strain rate test data, and it quotes the theoretical values calculated using Equation 1 ($t = 1$, $n \log t = 0$). This comparison shows reasonably good agreement for the constant-load data, and lesser agreement for the values derived from constant strain rate tests.

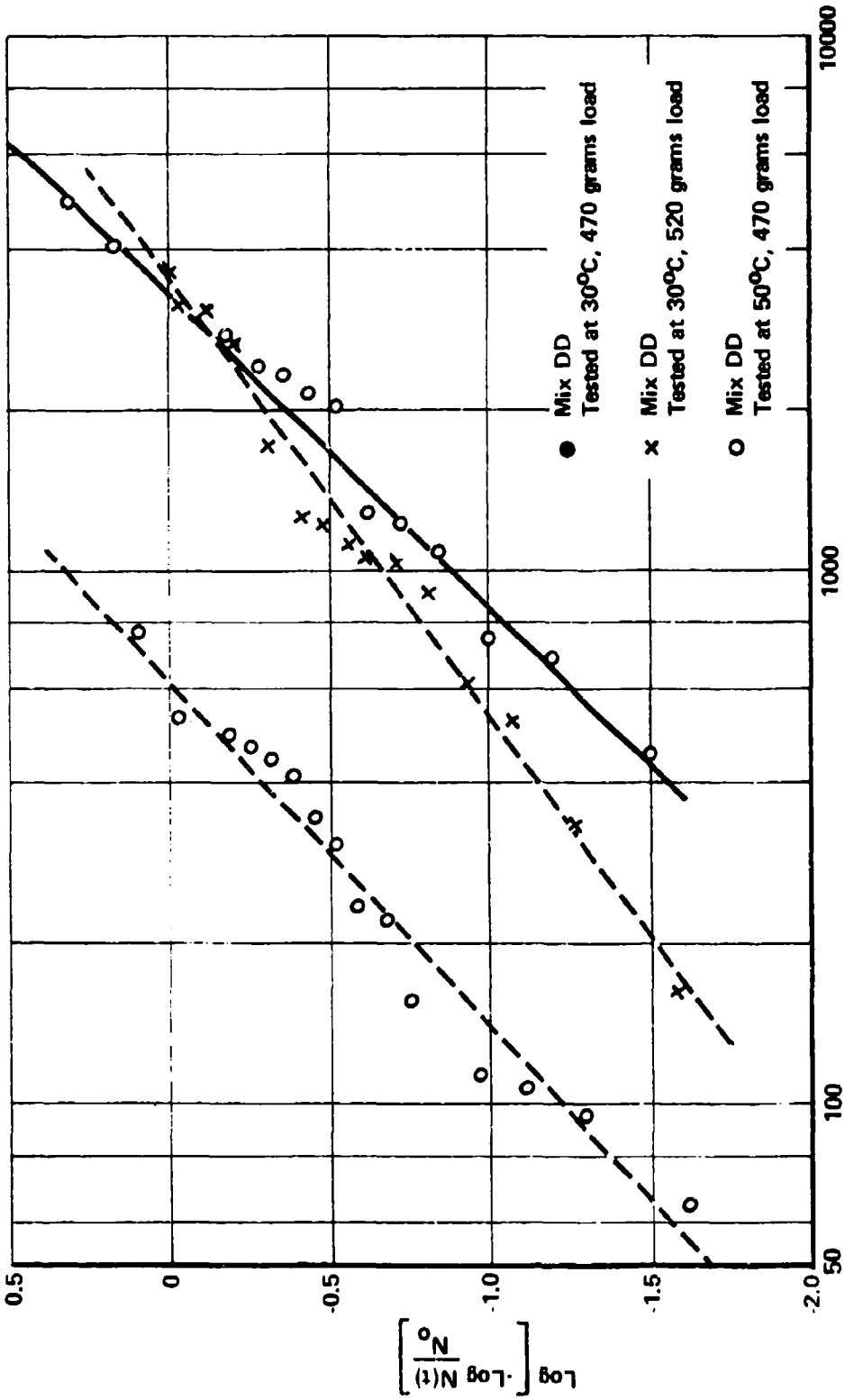

Figure 3-5 Data Plot, Creep Failure Distribution AlH_3/TVOPA Propellant

Table 3-2

WEIBULL PARAMETERS, COLD STORED
AlH_3/TVOPA PROPELLANT

Test Temperature (°C)	Applied Load					
	41 psia			46 psia		
	k, min ^{1}	n	t_b^{50}, min	k, min ^{1}	n	t_b^{50}, min
30	4.3×10^{-4} (0.988)	1.4	2,700	5.8×10^{-4} (0.989)	1.2	1,670
50	2.8×10^{-3} (0.976)	1.4	300	--	--	--

( ) = Coefficient of Correlation, Linear Regression of Weibull Data Plots

Table 3-3

SHIFT FACTORS AND NORMALIZED RATE CONSTANTS
COLD STORED AlH_3/TVOPA PROPELLANT

WLF Temperature-Time Shift Factors

^{0}C	10	30	50	70
a_T	1.00	6.89×10^{-2}	6.17×10^{-3}	1.09×10^{-3}

Stress-Time Shift Factor

	Values Derived From Constant-Load Creep Tests	Values Derived From Constant Strain Rate Tensile Tests
$\sigma(\infty)\frac{286}{T}$	20 psia	30 psia
$\sigma(1)\frac{286}{T}$	483 psia	602 psia
η	--	2.66

Agreement of Extrapolated Values For k_o with Theoretical Values

n	1.2	1.4	0.8
k_o, Test Data Extrapolation	4.1×10^{-1}	6.4×10^{-1}; 5.1×10^{-1}	0.12 ± 0.05
k_o, Theoretical	7.4×10^{-1}	7.7×10^{-1}	0.63
	Constant-Load Creep Failure Test		Constant Strain Rate Tensile Tests

Strain Rate Shift Factor

$a_{\dot{\epsilon}} = 8.97 \times 10^{-5}\ min^{-1}$

(2) Aged Propellant. Constant-load fatigue testing of the AlH_3/TVOPA propellant was repeated after 574 days storage at 20 and 30°C. The results were as follows:

- Aging the propellant for 574 days at 20°C had no significant effect upon constant-load fatigue behavior. The distribution of failures remained unimodal, and the values of k and n remained the same within experimental error (Table 3-4). The data evidence that extended storage at 20°C caused neither binder degradation, as would be reflected in an increase in k, nor void formation, as would be reflected in an increase in n.

- Aging under 30°C produced a bimodal distribution of failures, and an increase in the values for both n and k (Table 3-4, Figure 3-6). The data imply that 30°C aging caused a degradation in binder properties reflecting in an increase in k values, and the development of physical damages (dewetting, gasing voids) reflecting in an increase in n values.

The data are compatible with the results of the uniaxial tensile tests, off-gas and X-ray analyses, all indicating a high sensitivity of the system to storage at temperatures in excess of 20°C. The constant-load fatigue failure data, moreover, reveal the large effect of this combination of reduced binder strength and increasing defect size upon failure distributions. To further illustrate this point, Table 3-4 quotes calculated times to failure for an initial sample size N_o = 100 under 41 psia combined (internal gas pressure and thermal stress) load at 30°C. The data show the severe degradation of load sustaining capability of this system at storage temperatures in excess of 20°C.

Summary. Catalytic gas scavenger systems were shown to be effective in suppressing internal hydrogen gas pressure build-up in AlH_3/TVOPA propellants under 20 to 30°C storage, and the catalysts were shown to remain active after 400 days.

The scavenger containing formulations produce small quantities of other gaseous species, notably CO_2, that are attributable to TVOPA decomposition or interaction with AlH_3 or AP. The rate of generation of these gases is negligible at 20°C but increases rapidly with increasing temperature to cause a serious shelf-life limitation at storage temperatures of 30°C and above. Degradation of the TVOPA further produces moisture and HF to cause degradation of the polyester binder polymer; as a result, propellant stored at 30°C or higher temperatures show failures within 1½ to 2 years as a result of internal gas pressure and loss in binder stress capability.

A properly stabilized AlH_3/TVOPA propellant stored at temperatures of 20°C or below is expected to have an average shelf-life in excess of 3 years, however, with considerable batch-to-batch variability. This variability in part, is caused by AlH_3 surface attrition during mixing, and the problem

Table 3-4

AlH_3/TVOPA PROPELLANTS, EFFECT OF AGING UPON FAILURE DISTRIBUTIONS

	Calculated Times to Failure, Minutes No = 100				
	First Failure	First 10%	First 20%	50%	100%
Cold-Box Stored Propellant $k = 4.3 \times 10^{-4}$ min^{-1} n = 1.4	87	465	796	1789	6920
Aged 574 Days at 30°C $k = 3.5 \times 10^{-3}$ min^{-1} n = 8.23	163	217	238	242	343

Test Conditions: 41 psia Load, 30°C

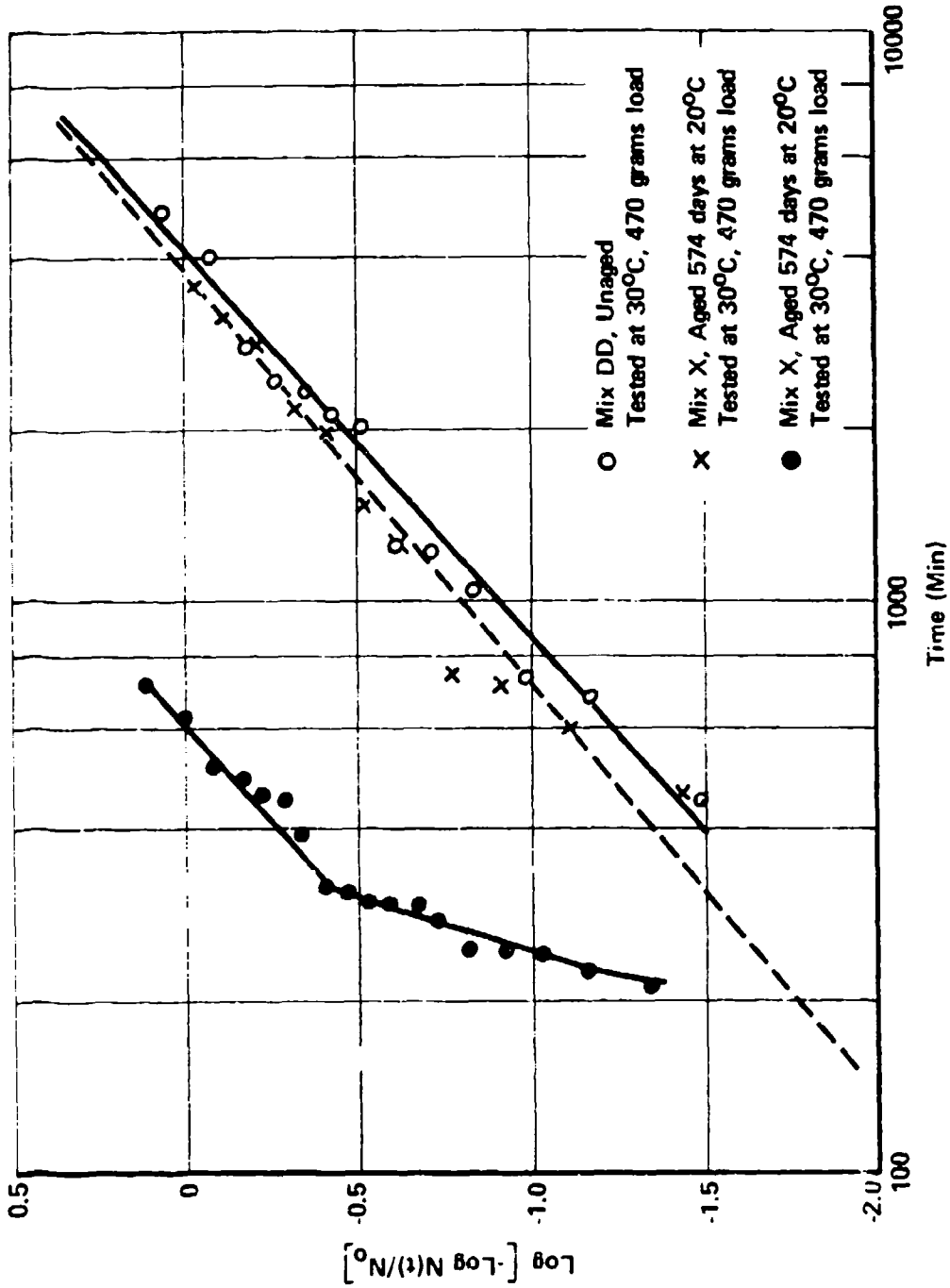

Figure 3-6 Creep Failure Distribution, Aged AlH$_3$/TVOPA Propellant

increases in severity as solids loading is increased. This poses a prohibitive process and quality control problem.

A detailed assessment of AlH_3/TVOPA motor service life would require the definition of motor internal stress conditions as a function of storage temperature and time, and a definition of the rate of decreasing propellant stress capability as a function of temperature and internal gas pressure-induced fatigue. This is shown schematically in Figure 3-7. The projected distribution of failures is given by the intersect plane as schematized in Figure 3-8. Such more detailed analyses were not performed since range calculations showed that AlH_3/TVOPA propellants would produce only limited gains notably if weighed against anticipated problems in attaining service life reproducibility.

3.2.2 PCDE Propellants

PCDE is a binder polymer of more recent development that can be plasticized with nitrate esters or derivatives of aliphatic nitro compounds for use in aluminized composite propellants. These propellants afford density specific impulse values that render them attractive for upper stage ballistic missile application.

PCDE contains fluorine, and depending upon manufacturing methods, the material may contain small, but nevertheless significant quantities of chemically unstable or reactive impurities that may impair propellant thermal stability and service life. This program was to assess this situation, using both a model PCDE propellant and a ballistically optimized system. The model propellant used di-n-butyl phthalate as the plasticizer to render propellant stability and service life capability to be largely a function of PCDE stability itself; the ballistically optimized system, contained a nitrate ester plasticizer to cause propellant stability to become a more complex function of materials stability and interactions.

3.2.2.1 Model PCDE Propellant

The model PCDE propellant was processed in 1-gallon Baker Perkins mixer and vacuum cast into 30 cm length elliptical tube specimens for storage at 40 and 60°C. The tubes were X-rayed periodically, and propellant cut from the center section was used to determine uniaxial tensile properties and constant-load failure distributions as a function of storage time. Off-gas evolution rates were determined with propellants and pure polymer sealed and stored in glass ampules.

Propellant Surveillance. There were no failures as detectable by X-ray upon storing the propellant in the form of elliptical tube specimens for 181 days at 40 and 60°C. The results imply that even at 60°C gas generation rates are below the level that would cause cracking at web thicknesses below 15 cm.

Off-Gas Analyses: PCDE Polymer. The off-gassing rates for two lots of PCDE polymer were determined over the 60 to 100°C temperature range.

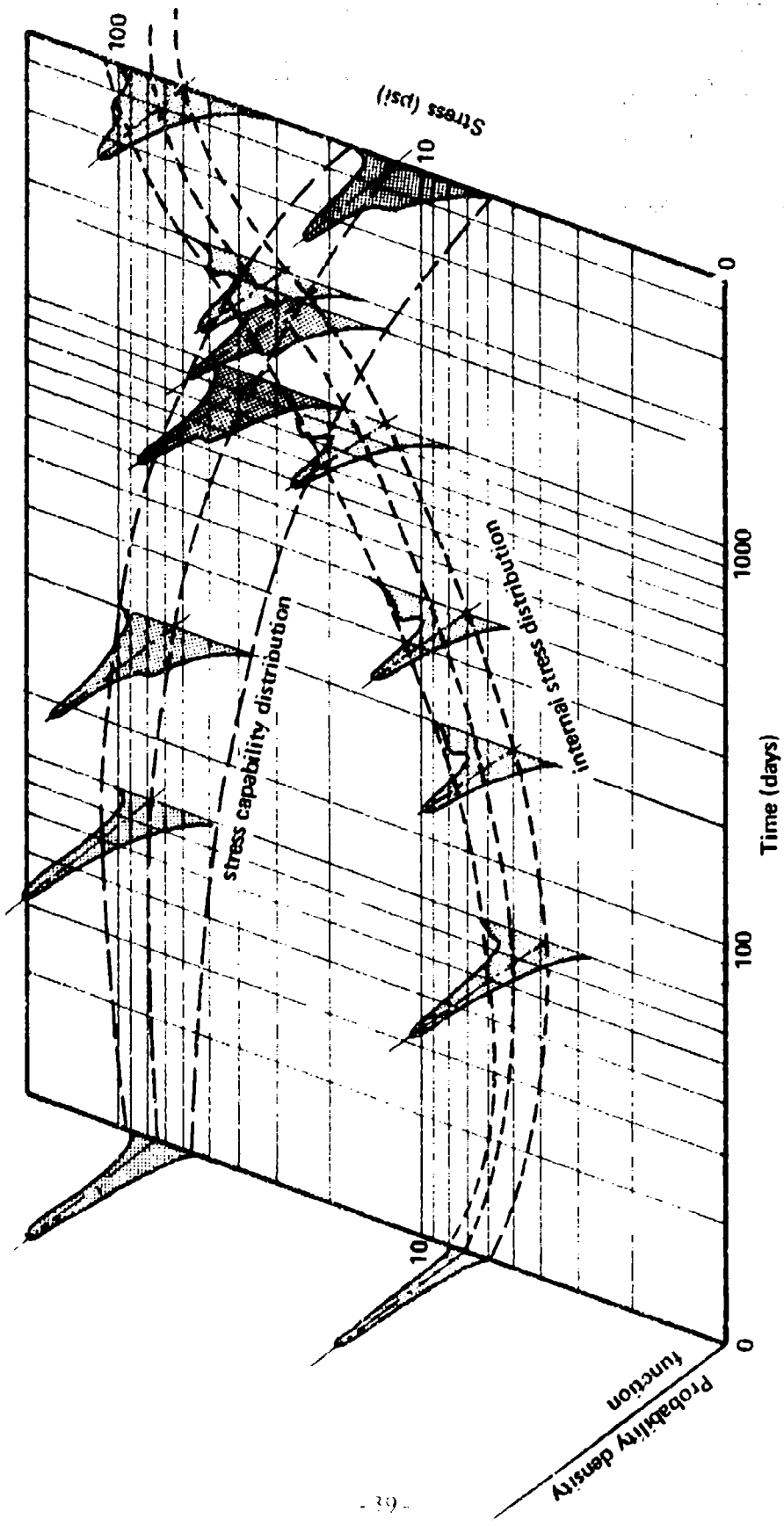

Figure 3-7 Distribution of Motor Internal Stress/Pressure versus Propellant Stress Capability (Schematics)

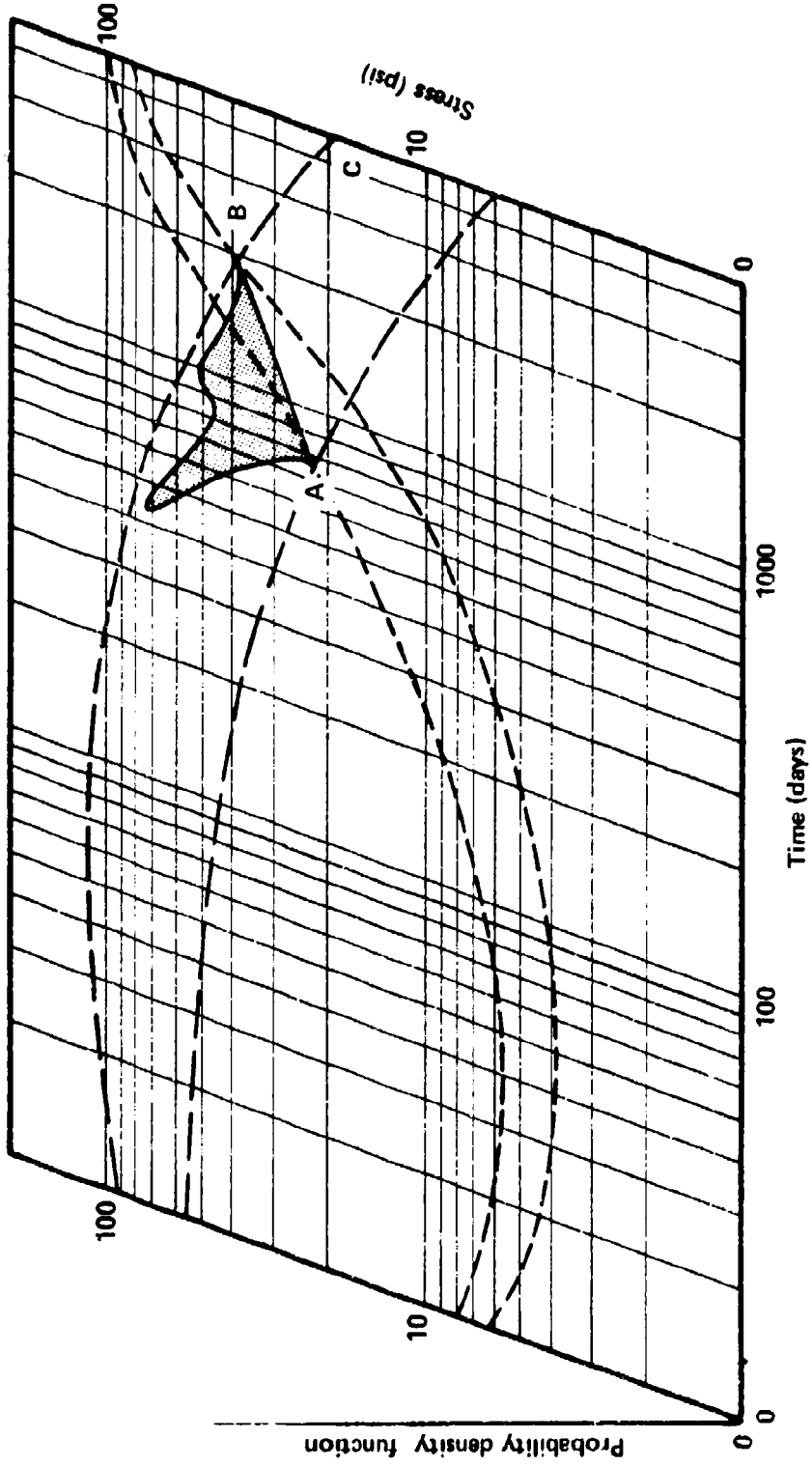

Figure 3-8 Projected Inventory Failure Distribution (Schematics)

The dominant species were CO_2, CO, N_2, and N_2O, besides H_2O, HF, HCN, $(CH_2)_x$ and NO. With both lots gas evolution rates decreased with time to indicate residual impurities as the gas source. Gas generation data for both the PCDE polymer and the propellant are quoted in Table 3-5. These data, showing no gross discrepancy between polymer and propellant, suggest that there does not exist any gross incompatibility in the propellant.

Figure 3-9 gives Arrhenius plots of the gassing data, and Table 3-6 quotes the Arrhenius parameters. The data suggest that one mechanism may be responsible for the production of CO_2, CO and N_2 with Lot 12260-44, while the decomposition mechanism of Lot 169 appears to be more complex. Data scatter for the N_2 production by Lot 169 prevented quotation of rate data.

Uniaxial Tensile Properties. The uniaxial tensile properties were determined using mini-thin tensile specimens prepared under controlled humidity environment.

The zero-time test data are presented in the form of a failure envelope in Figure 3-10. Temperature-reduced stresses at break versus temperature-reduced times to break are shown in Figure 3-11; the median time to break under constant load falls on the curve for the constant strain rate data which suggests that the stress-time shift factor should be the same for either condition.

Tensile test data as a function of aging time at 40 and 60°C are shown in Figure 3-12; there is a decrease notably in the maximum stress values through 120 days storage, followed by a recovery. The mechanism that could cause this recovery is not understood.

Constant-Load Fatigue (Creep-Failure) Test. Freshly processed propellant and propellant cut from the center of the tubes was used to determine failure distributions under constant load as a function of storage time at 40 and 60°C. The data, in terms of the parameters of the expanded Weibull failure distribution function (Equation 4) are summarized in Table 3-7. Limitations in PCDE polymer supply restricted the available number of tubes and thereby the number of specimens that could be used to approximately 20 per test; with samples affording multi-modal distributions this impairs the accuracy of the data. A typical Weibull plot of raw data (unaged propellant), and of the reconstructed data using the derived values for the sub-populations, is shown in Figure 3-13. Additional test data plots showing the effect of 60°C aging upon creep failure distributions are shown in Figure 3-14. Figures 3-15 and 3-16 present plots of the parameters of the expanded Weibull distribution as a function of aging time at 40 and 60°C. These data, in agreement with the uniaxial tensile test data, show a reversal in trend after 120 days aging at either temperature.

There was not enough of the propellant available to perform additional tests at different temperatures and loads to derive the parameters for the shift factors.

Kinetic Analysis, Constant Strain Rate Tensile Data. Constant strain rate tensile tests conducted with unaged model PCDE propellant over the 20

Table 3-5

OFF-GAS VOLUMES, PCDE POLYMER AND MODEL PROPELLANT

Micromoles/Gram

		CO_2	CO	N_2	N_2O
PCDE Polymers					
100°C	300 Hours	100/100	30/30	40/40	4/6
	600 Hours	130/ 160	35	50	7/>7
80°C	300 Hours	22/25	4/4	8/9	1/1
	600 Hours	36	7	9	2/>2
60°C	600 Hours	15/11	1/3	3/3	1
	3200 Hours	31	5	8 At 2400 Hours	4 At 2400 Hours
Model PCDE Propellant[1]					
60°C	600 Hours	27	1	4	Trace
	1600 Hours	31	4	6	Trace

(1) Data restated on polymer weight basis

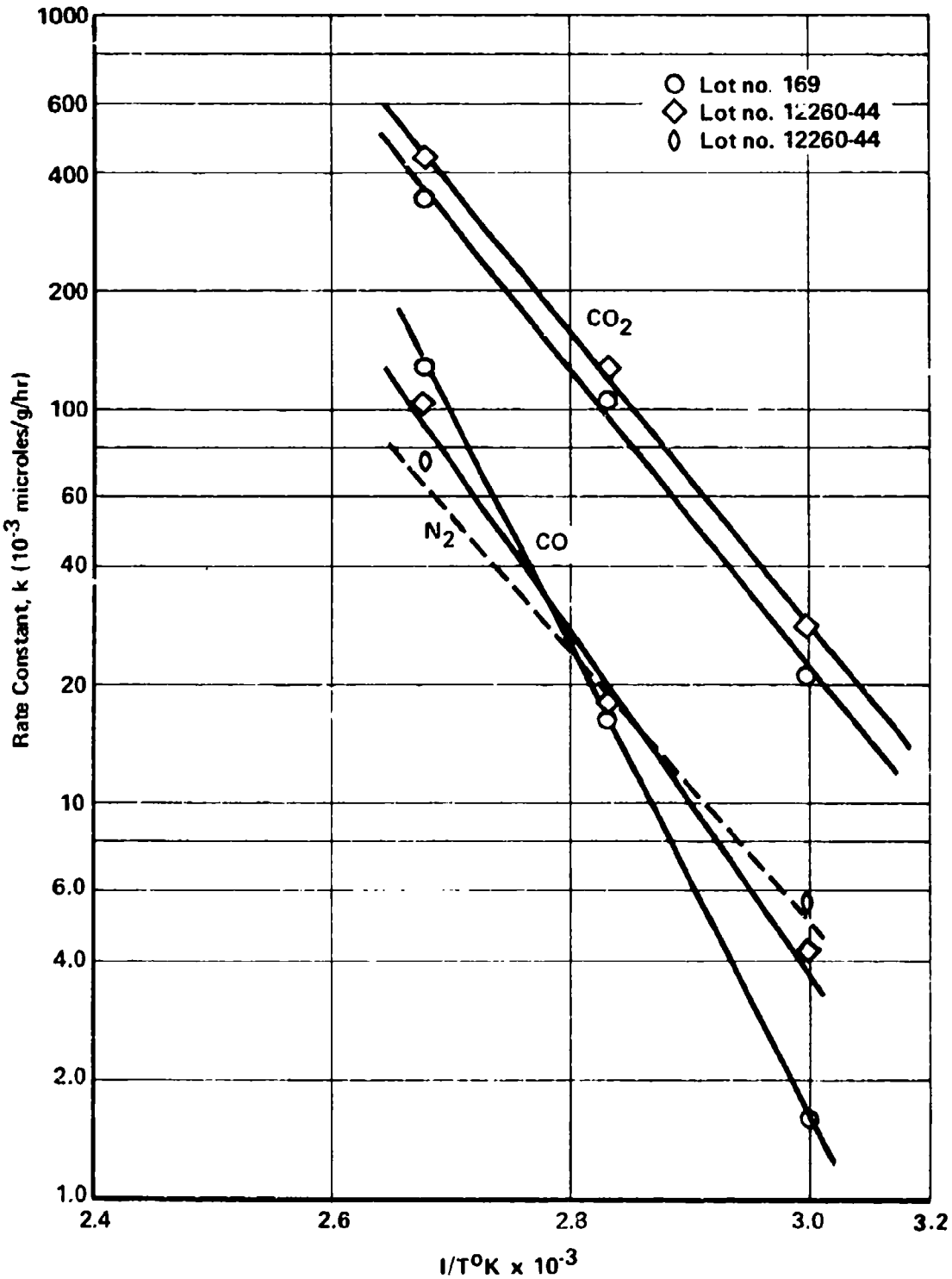

Figure 3-9 Arrhenius Plots of CO_2, CO and N_2 Gassing Rates

Table 3-6

PARAMETERS OF THE ARRHENIUS RATE EQUATIONS[a]

PCDE LOT NO.	E (KCAL)	LOG A	A
CO_2			
169	17.27	9.763	5.79×10^9
12260-44	17.05	9.555	3.59×10^9
CO			
169	27.19	15.028	1.067×10^{15}
12260-44	19.76	10.052	3.32×10^{10}
N_2			
12260-44	15.95	8.150	1.414×10^8

(a) Initial rates of gas generation

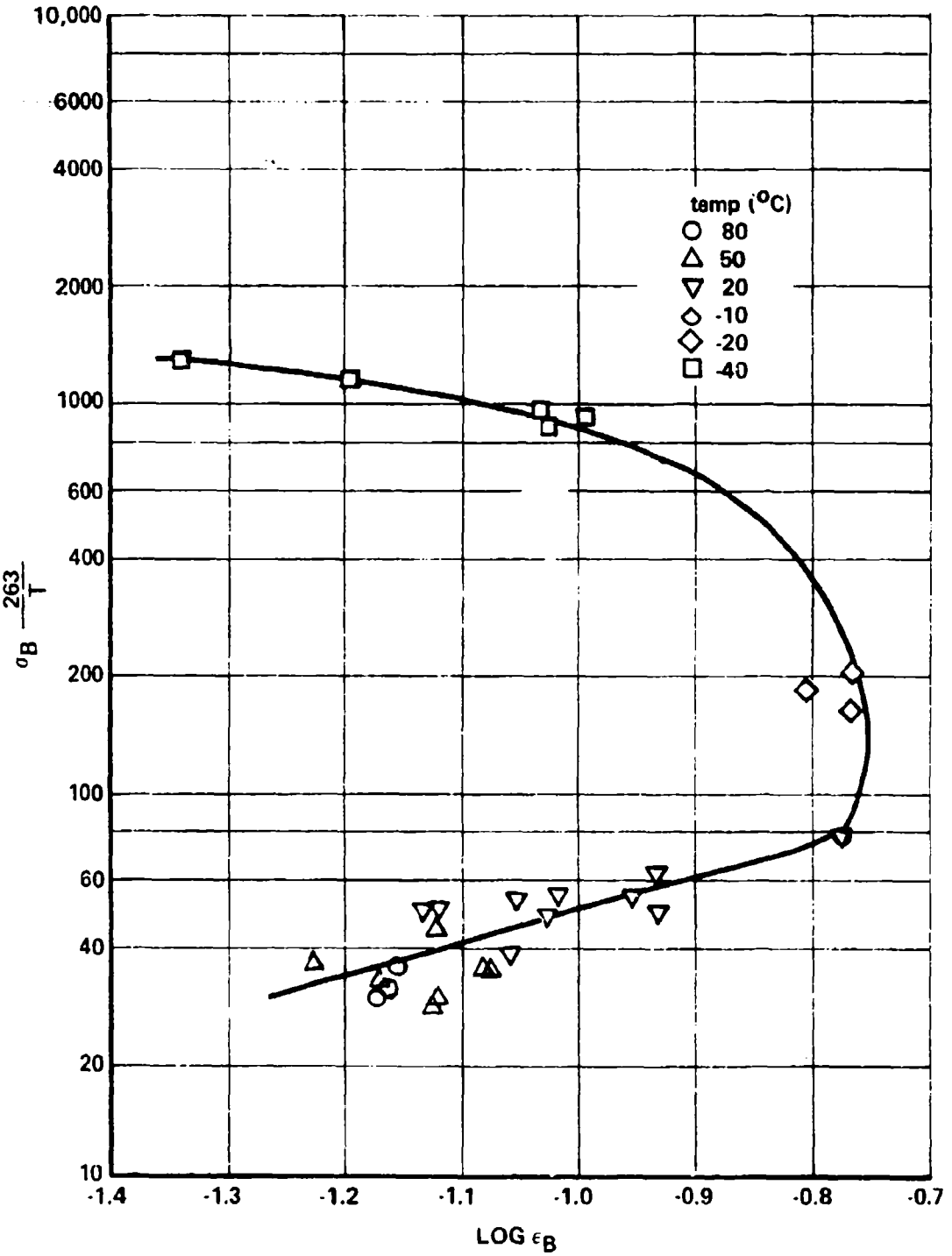

Figure 3-10 Failure Envelope - PCDE Control Propellant Mix 0152-16-1E

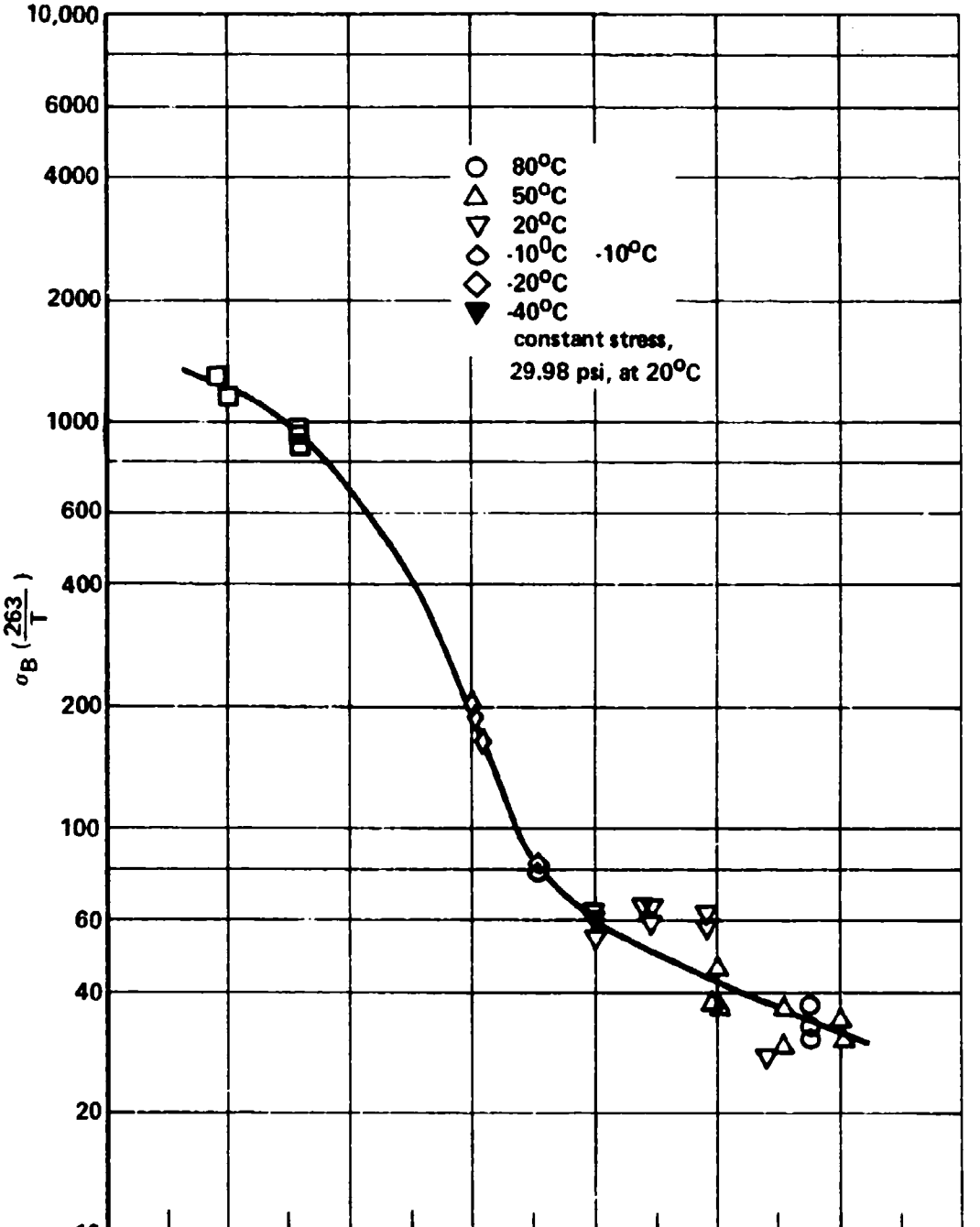

Figure 3-11 Master Curve - Stress at Break PCDE Control 0152-16-1E

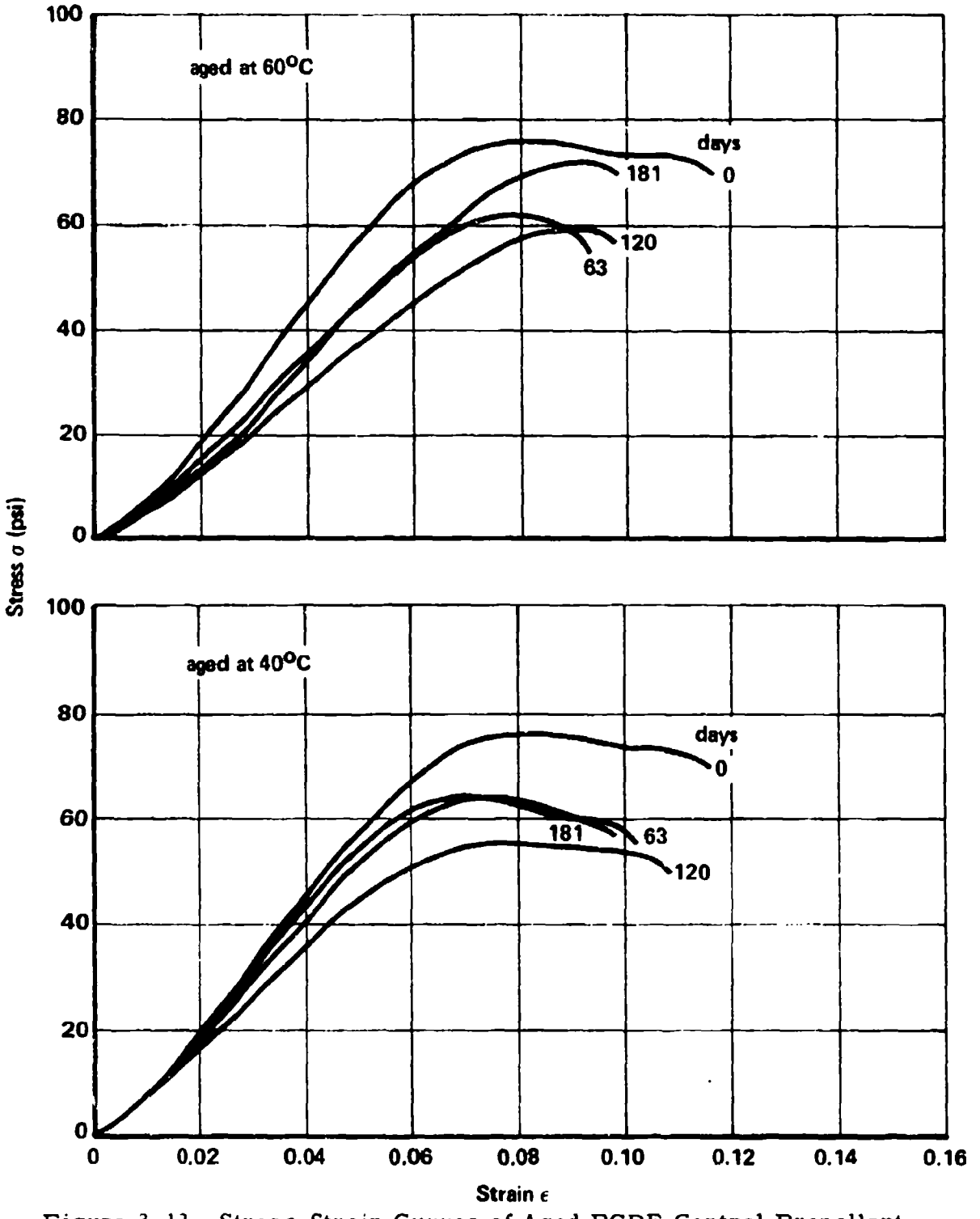

Figure 3-12 Stress-Strain Curves of Aged PCDE Control Propellant (0152-16-1E). Stress-Strain Curves Recorded at 20°C and 0.108 min^{-1}.

Table 3-7

MODEL PCDE PROPELLANT

Constant-Load Fatigue. 30 psia, 30°C

	Expanded Weibull Parameters					
	Sub-Population 1			Sub-Population 2		
	α_1	k_1, min^{-1}	n_1	α_2	k_2, min^{-1}	n_2
60°C Aging						
1. Unaged	0.47	8.3×10^{-4}	2.4	0.53	2.5×10^{-3}	2.5
2. 60 Days	0.3	1.0×10^{-1}	2.9	0.6	1.8×10^{-1}	7.6
3. 120 Days	0.5	2.7×10^{-1}	6.8	0.4	4.6×10^{-1}	13
4. 181 Days	0.45	5.2×10^{-2}	6.0	0.55	1.3×10^{-1}	3.0
40°C Aging						
1. 60 Days	0.45	1.0×10^{-1}	2.4	0.55	1.2×10^{-1}	1.3
2. 120 Days	0.6	1.1×10^{-1}	2.7	0.4	1.9×10^{-1}	1.7
3. 180 Days	0.5	0.6×10^{-1}	9.7	0.5	1.5×10^{-1}	3.2

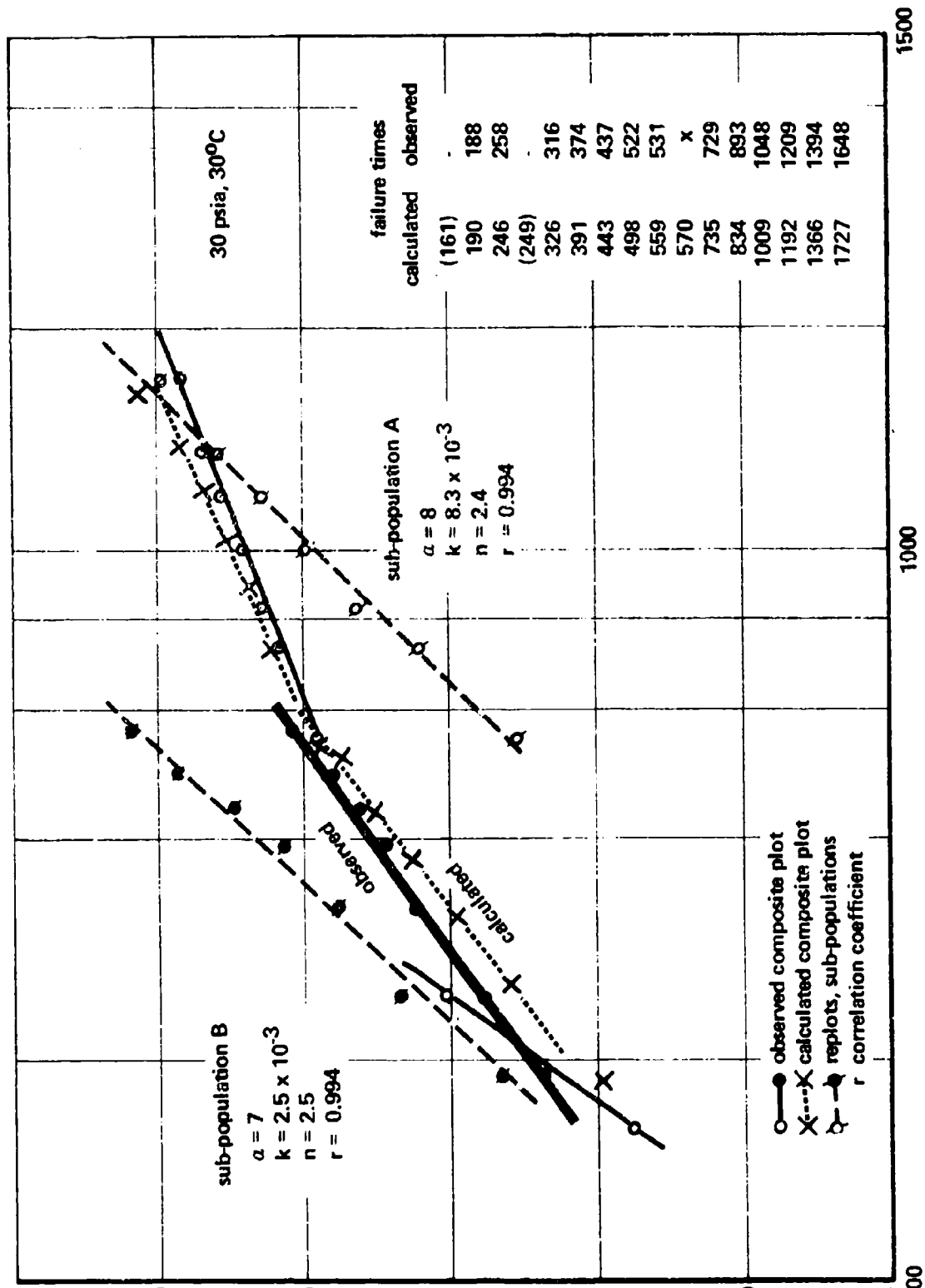

Figure 3-13 Weibull Plot, Creep-Failure Data, Unaged Model PCDE Propellant

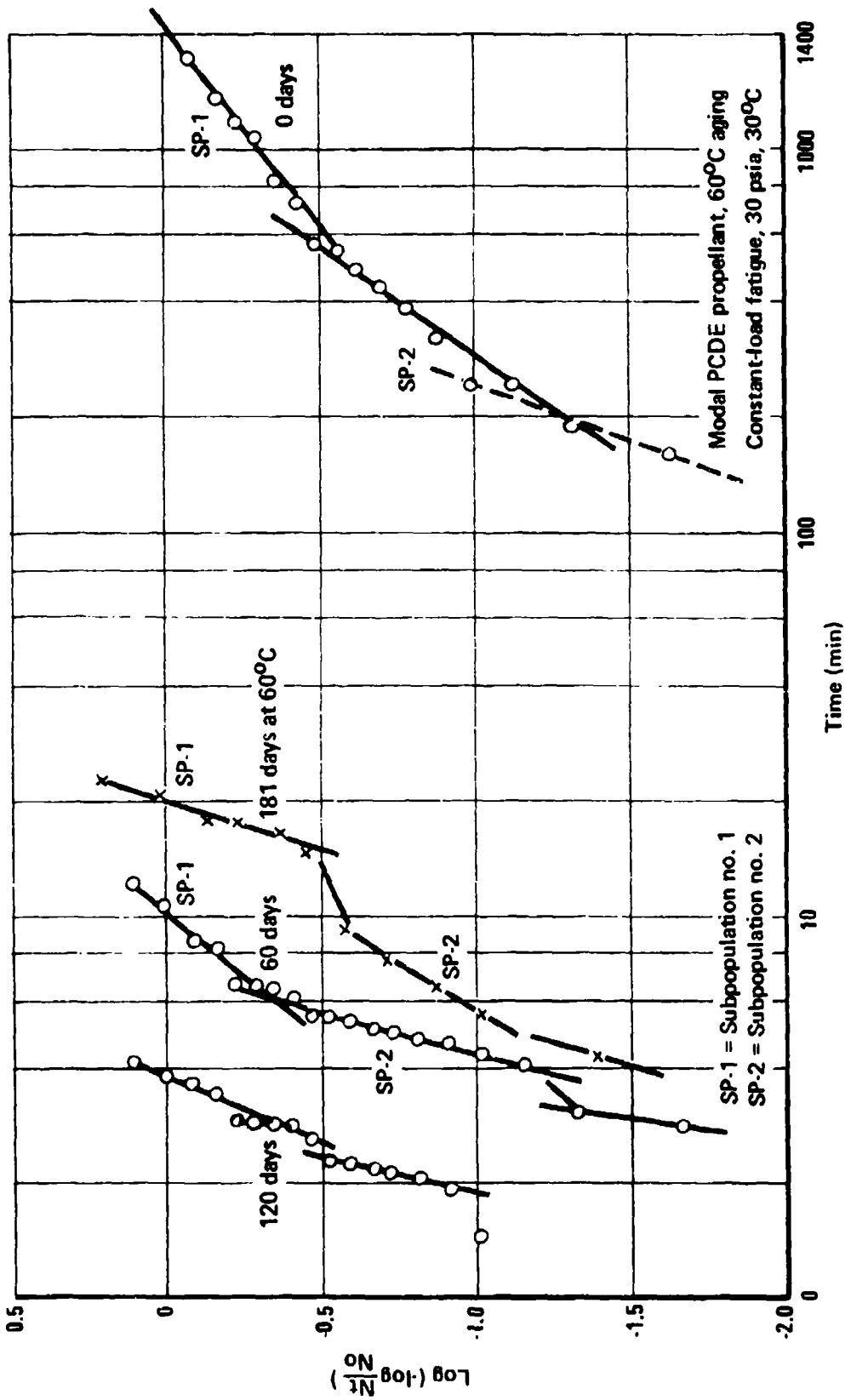

Figure 3-14 Weibull Plots, Creep-Failure Data, Model PCDE Propellant, 60°C Aging

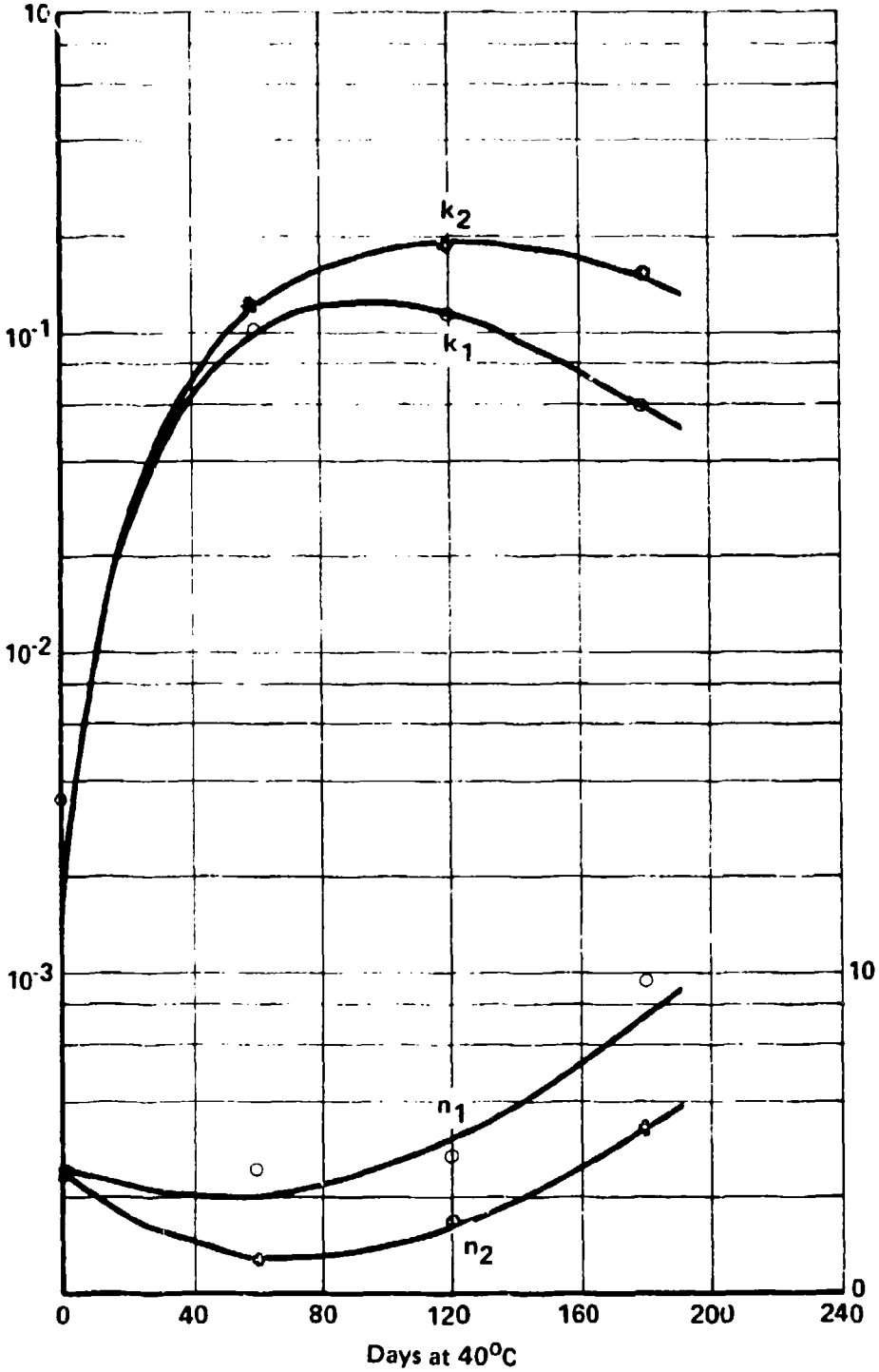

Figure 3-15 Expanded Weibull Parameters, Model PCDE Propellant Aged at 40°C

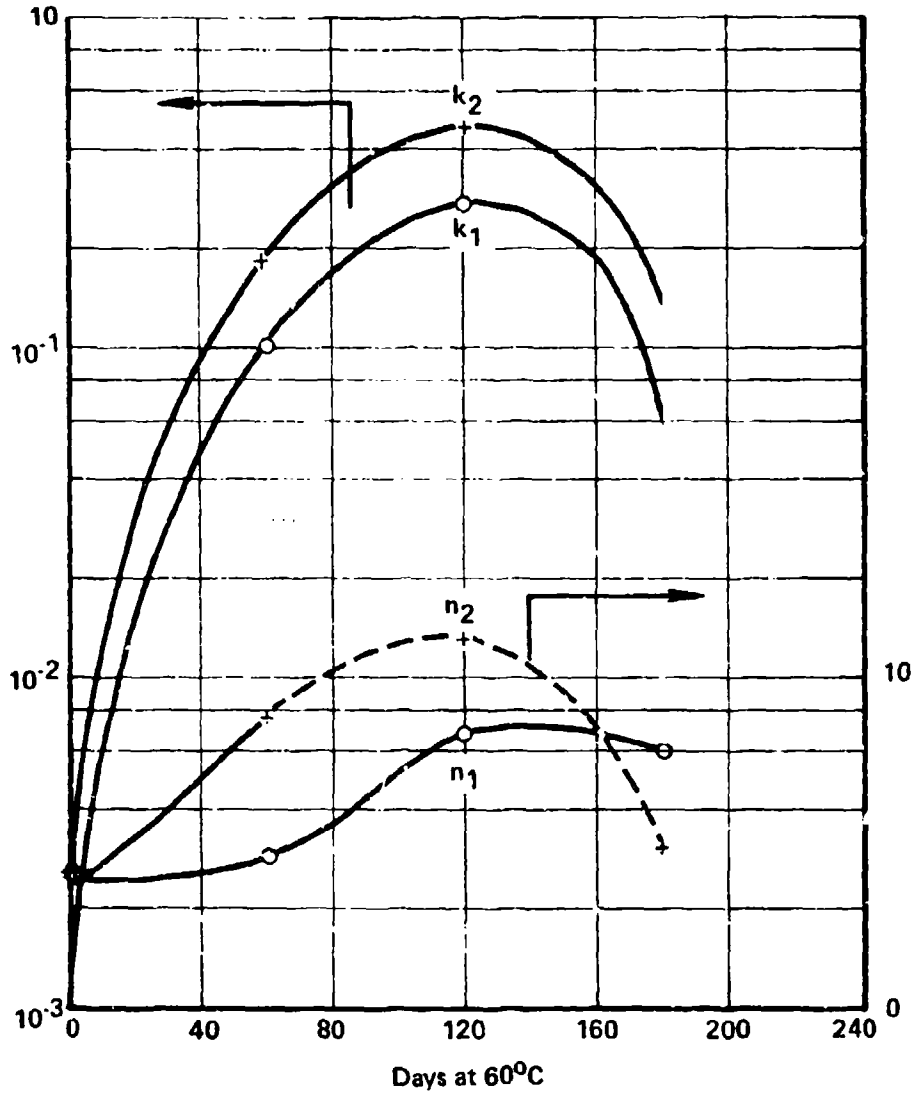

Figure 3-16 Expanded Weibull Parameters, Model PCDE Propellant Aged at 60°C

to 80°C temperature range produced the data summarized in Table 3-8. Using the k_o value derived from these data, and the appropriate values for the temperature-time and the stress-time shift factors to calculate the value for the rate constant at 30°C, 30 psia, yields 7.9×10^{-4} min^{-1}. Treating the constant-load creep failure data as a single population affords a $k_{(30^0,\ 30\ psia)}$ value of 1.13×10^{-3} with a slope of $n \approx 1.4$. This constitutes a reasonable agreement between the k values determined by the creep failure test, and the k value derived by extrapolation of the constant strain-rate data.

Constant strain rate tensile tests conducted at 20°C and 0.108 min^{-1} strain rate on model PCDE propellant aged for varying times at 40 and 60°C produced the data quoted in Table 3-9. The data indicate that the critical stress, σ_{cr}, first decreases, then increases with storage time. As a result, a new set of parameters ($\sigma_{o(\infty)}$, $\sigma_{o(i)}$) would need to be generated to establish a_{ij}. Since test data were available at one strain rate only, the values for $\sigma_{o(\infty)}$ could not be determined; this, in turn, prevented the calculation of the rate constants for comparison with the constant-load creep failure test data.

The high value for $\sigma_{o(i)}$ quoted in Table 3-8 results from a break in the data plot used for determining the exponent of the power law for the stress-time shift factor, and from the extrapolation of the data plot beyond the break point into a regime that has no practical significance.

The significance of these results is that chemical aging appears to affect the parameters governing the stress-time shift factor.

Table 3-10 quotes the network moduli (E_{m1}, E_{m2}) and maximum extensibilities (λ_{m1}, λ_{m2}) derived from the constant strain rate test data. Although there is considerable data scatter, this tabulation nevertheless shows the same reversal in polymer network properties as is indicated by the constant load fatigue data plots (Figures 3-15 and 3-16). The data also indicate that the values for σ_{cr} follow the same trend. The data suggest that the values for k, E_{m2} (network modulus) and σ_{cr} may be dependent upon one common parameter relating to polymer structure.

Summary. The off-gas analyses and the mechanical test data indicate that the aging behavior of the model PCDE propellant is dominated by two processes. During the initial 100 to 120 days aging at either 40 or 60°C, there appears to be some polymer degradation accompanied by gassing and resulting in softening; during this time period both the scale and the shape parameters of the expanded Weibull creep failure distribution increase to cause a rather drastic shift in failure distributions toward shorter times. This may be attributed to the presence of a thermally unstable, structural irregularity in the PCDE polymer.

After this initial aging period, characterized by gassing and softening, the propellant hardens as evidenced by both uniaxial tensile and creep test data. This may be attributed to a secondary cross-link process which may be catalyzed by some of the early products of polymer degradation. This process could be more intimately associated with the basic structure of the polymer as opposed to being caused by impurities.

Table 3-8

UNAGED MODEL PCDE PROPELLANT, KINETIC ANALYSIS OF CONSTANT STRAIN RATE TENSILE DATA

T (°C)	$\dot{\epsilon}$ (min^{-1})	σ_B (psi)[1]	ϵ_B	$\sigma_2(\infty)$[2]	θ (min)	n	k_o (min^{-1})
80	0.00108	41.84	0.06875	22.44	43.280	0.577	0.475
50	0.0108	55.61	0.07535	24.10	0.9753	0.679	1.164
20	0.108	60.20	0.11140	30.71	0.1725	0.872	0.856
		66.12	0.11729	29.83	0.2566	0.697	0.890
	0.0108	60.45	0.09637	30.26	2.1147	0.854	0.993
		53.77	0.09362	32.60	1.9720	1.024	1.747
		60.39	0.08854	32.96	3.3704	0.719	0.946
Avg.						0.77	1.02
Std Dev.						0.15	0.38

Stress-Time Shift Factor		Temperature-Time Shift Factor	a_T
$\sigma_{o(\infty)}$	18 psia	T_s = 10°C	1.0
$\sigma_{o(1)}$	1540 psia	20°C	9.556×10^{-3}
$1/\bar{n}$	2.66	30°C	3.142×10^{-3}
		50°C	5.133×10^{-4}
		80°C	6.890×10^{-5}

Strain Rate Shift Factor

$\dot{\epsilon}_o = 1.160 \times 10^{-5}$ min^{-1}

(1) True stress

(2) Onset of flaw or crack growth step; $B \leq 1$

Table 3-9

KINETIC ANALYSIS OF AGED PCDE CONTROL PROPELLANT (0152-16-1E) UNIAXIAL STRESS-STRAIN CURVES RECORDED AT 20°C AND 0.108 MIN^{-1}

Aged					
T (°C)	Days	σ_b (psi)[1]	ϵ_b	$\sigma_2(\infty)$[2]	θ (min)
40	63	53.98	0.10595	20.81	0.1485
		47.79	0.10378	20.49	0.2298
		55.53	0.10378	22.61	0.1989
	120	42.33	0.10216	16.32	0.1072
		39.26	0.10865	17.85	0.1134
		44 36	0.12757	24.49	0.3595
	181	51.13	0.09784	24.56	0.1779
		51.49	0.08108	27.78	0.2882
		56.03	0.08973	31.36	0.1792
60	63	55.14	0.09297	16.85	0.0377
		52.65	0.10162	15.76	0.1456
		49.96	0.09081	19.28	0.0952
	120	52.64	0.09784	20.40	0.3048
		57.50	0.10432	10.84	0.0611
	181	50.69	0.08973	23.48	0.1846
		54.45	0.09730	21.65	0.1721
		51.62	0.09946	29.86	0.1965

(1) True Stress; $\sigma = \sigma_c (1 + \epsilon)$.

(2) Crack Growth Step.

Table 3-10

NETWORK PARAMETERS AND LONG-TERM STRESS OF AGED PCDE CONTROL PROPELLANTS, NO. 0152-16-1E

Measurements Taken at 20°C and 0.108 min^{-1}

Aged						
T (°C)	Days	$E_1 \frac{263}{293}$ (psi)	λ_1	$E_2 \frac{263}{293}$ (psi)	λ_2	$\sigma_{(\infty)} \frac{263}{293}$ (psi)
	0	16.10 - 19.44	1.0209 - 1.0229	132.76 - 200.62	1.1085 - 1.1597	26.77 - 27.56
40	63	12.45	1.0167	127.67	1.1132	20.81
		82.59	1.0780	113.82	1.1039	20.49
		12.41	1.0189	120.72	1.1103	22.61
	120	56.01	1.0555	117.43	1.1150	16.32
		10.56	1.0169	109.14	1.1127	17.85
		16.72	1.0294	134.19	1.1740	24.49
	181	13.18	1.0188	121.81	1.1036	24.56
		13.82	1.0168	192.67	1.1590	27.78
		(1)	(1)	191.63	1.1472	31.36
60	63	--	--	103.63	1.1080	16.85
		--	--	92.83	1.1040	15.76
		21.81	1.0302	107.53	1.1197	19.28
	120	20.22	1.0292	116.43	1.1436	20.40
		--	--	96.26	1.1141	10.84
	181	--	--	185.66	1.1657	23.48
		--	--	128.12	1.1290	21.65
		--	--	187.96	1.1895	29.86

(1) Excessive data scatter.

Because of this reversal the existing data extending only through 180 days aging are not sufficient to accurately predict long-term aging behavior. Nevertheless, the Weibull data plots (Figures 3-15 and 3-16) suggest that the suspected secondary crosslink process will continue to operate past the 180-day aging period, and that it will do so even under moderate storage conditions.

The appearance of a bimodal creep failure distribution further suggests that the model propellant was non-uniform with respect to binder composition. This non-uniformity persisted throughout the aging period.

3.2.2.2 Ballistically Optimized PCDE Propellant

This propellant was received from Aerojet-General in the form of blocks and 30 cm long elliptical tube specimens which were placed into storage at 30, 40, and 50°C.

X-ray examination revealed failure by crack formation after 30, 60, and 109 days at 30°C (3 tubes), 22 and 30 days at 40°C (2 tubes), and after 15 days at 50°C (2 tubes). These data indicate a rather serious stability problem.

Off-Gas Analyses. Samples of the propellant were sealed into glass ampules and stored at 50°C for periodic off-gas analyses. The results are plotted in Figure 3-17. The most dominant gas species (75 mole percent) is CO_2, followed by N_2O, with lesser quantities of HCN, CO and H_2O being generated and released into the gas phase. The gas volumes appear to be compatible with the PCDE polymer off-gas data quoted in Table 3-5, and they are not indicative of any gross incompatibility problem. This appears to be in conflict with the results of the surveillance tests.

Uniaxial Tensile Properties. The uniaxial tensile properties (Table 3-11) reveal no gross deterioration during short-term storage at 30 and 40°C. Data scatter is attributable to defects present in some of the test specimens.

Constant-Load Fatigue (Creep Failure) Testing. Propellant cut from the center sections of the tubes was used to prepare mini-thin tensile specimens for determining constant-load failure distributions. The results of these tests, in terms of the parameters of the expanded Weibull distribution function (Equation 4) are summarized in Table 3-12. Raw data plots for the 40°C aging series are shown in Figures 3-18, 3-19, and 3-20. Figure 3-21 gives a plot of the change in the Weibull parameters with aging time at 30 and 40°C.

The data show a distinctly different aging behavior than was observed with the model PCDE propellant (Figures 3-15 and 3-16).

The failure distributions, again, are bimodal, the two sub-populations, however, differing more in the n values. In part this may be attributed to defects being present in the test specimens, and it could represent an artifact. Aging induced defects were particularly noticeable with the material aged for 30 days at 40°C, and this may account for the irregular plots for k_1 (40°C) and n_1 (40°C), even though obviously defective specimens had been discarded.

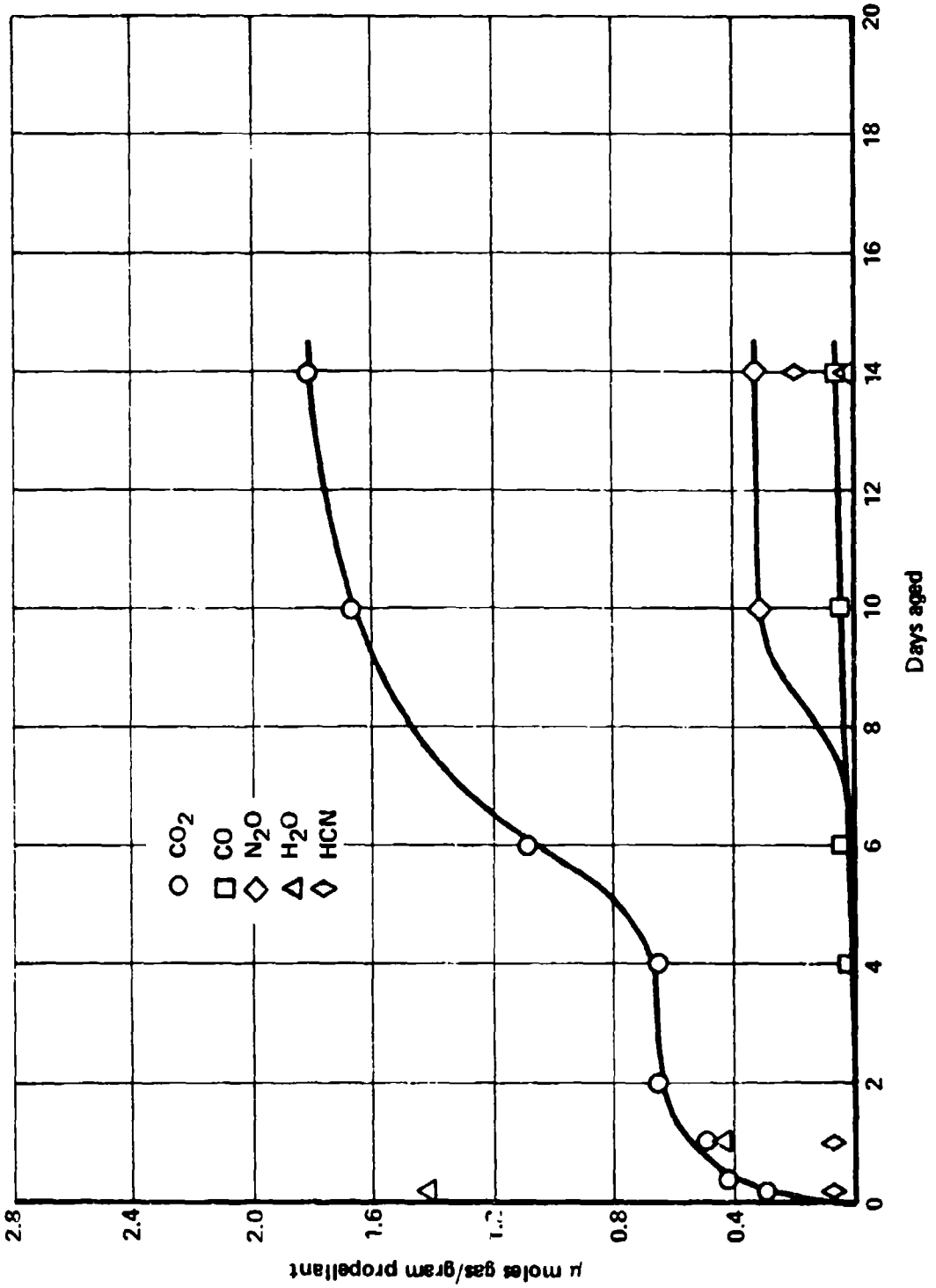

Figure 3-17 Propellant No. 73-05-245 Aged at 50°C Off-Gas Analysis

Table 3-11

UNIAXIAL TENSILE PROPERTIES, BASICALLY OPTIMIZED PCDE PROPELLANT[a]

Aging Condition		Test	Stress at	Strain at
Temperature	Time	Temperature	Break, psia	Break, %
Unaged	(b)	20°C	65/69/72	12/13/16
		35°C	49/56	15/20
		50°C	40/41	15/16
30°C	30 Day	20°C	68/76	13/13
	60 Day	20°C	67/59	13/13
40°C	22 Day	20°C	68/68	13/14
	30 Day	20°C	68	13

(a) Strain Rate 0.108 min^{-1}

(b) Excessive damage prevented testing at later times

Table 3-12

BALLISTICALLY OPTIMIZED PCDE PROPELLANT, CREEP FAILURE DISTRIBUTION

Aging Condition			Expanded Weibull Parameters					
			Sub-Population 1			Sub-Population 2		
Temperature (°C)	Time	Test Conditions	α_1	k_1 min^{-1}	n_1	α_2	k_2 min^{-1}	n_2
Unaged		23 psia, 21°C	0.42	7.6×10^{-4}	3.0	0.58	1×10^{-3}	1.7
		30 psia, 21°C	0.35	1.4×10^{-2}	1.8	0.55	5.2×10^{-3}	1.0
30	30 Days	23 psia, 21°C	0.38	5.4×10^{-4}	4.3	0.62	3.9×10^{-4}	0.9
	60 Days	23 psia, 21°C	0.45	2.6×10^{-3}	2.3	0.55	1.9×10^{-3}	1.0
40	22 Days	23 psia, 21°C	0.55	1.2×10^{-3}	1.4	0.45	2×10^{-3}	0.9
	30 Days[1]	23 psia, 21°C	0.54	0.8×10^{-3}	2.1	0.56	2.6×10^{-3}	0.8

(1) Test specimens selected to eliminate grossly defective specimens, and spurious data points ignored in the calculations.

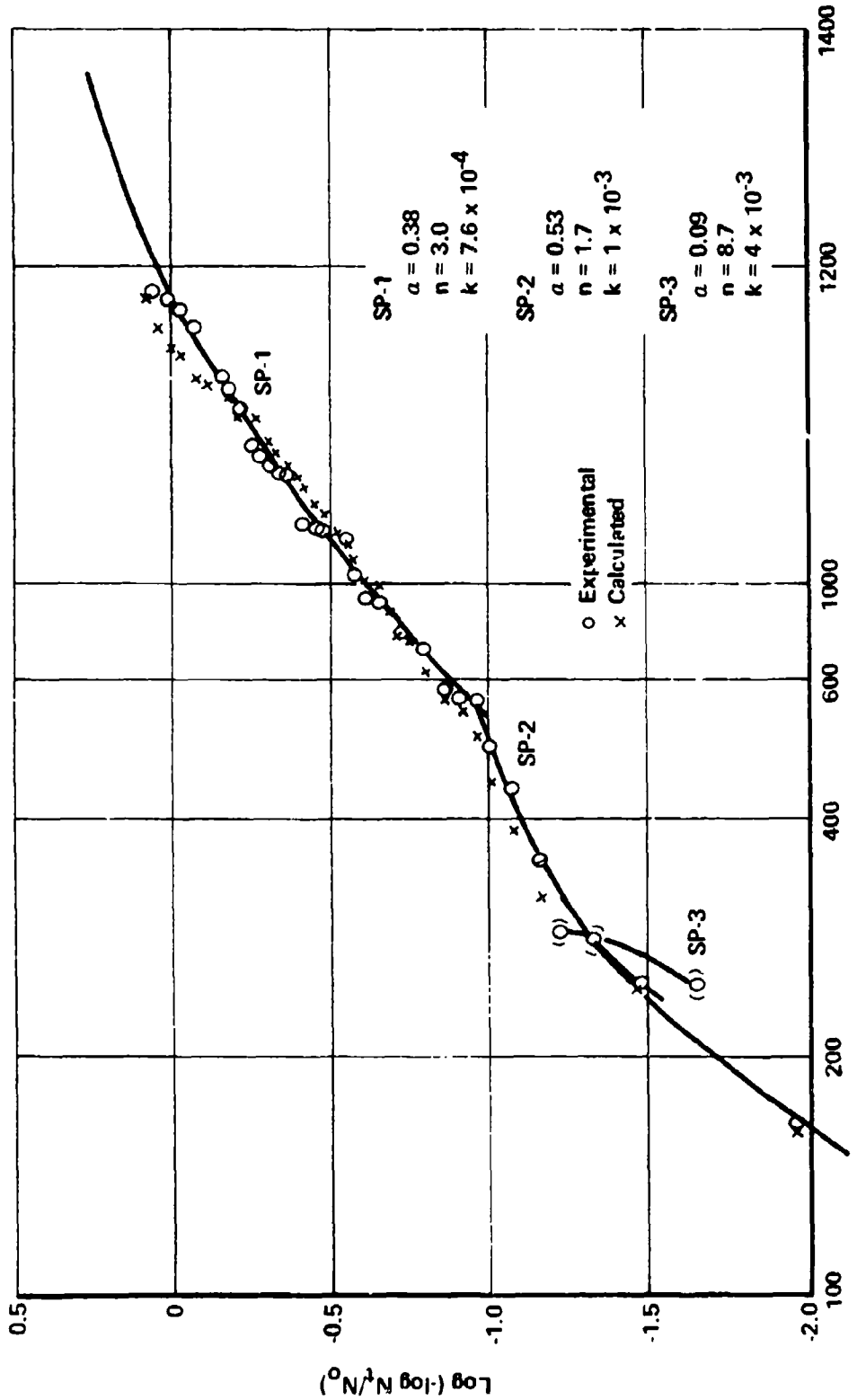

Figure 3-18 Ballistically Optimized PCDE Propellant, Zero-Time, 23.2 psia, 21°C (Air)

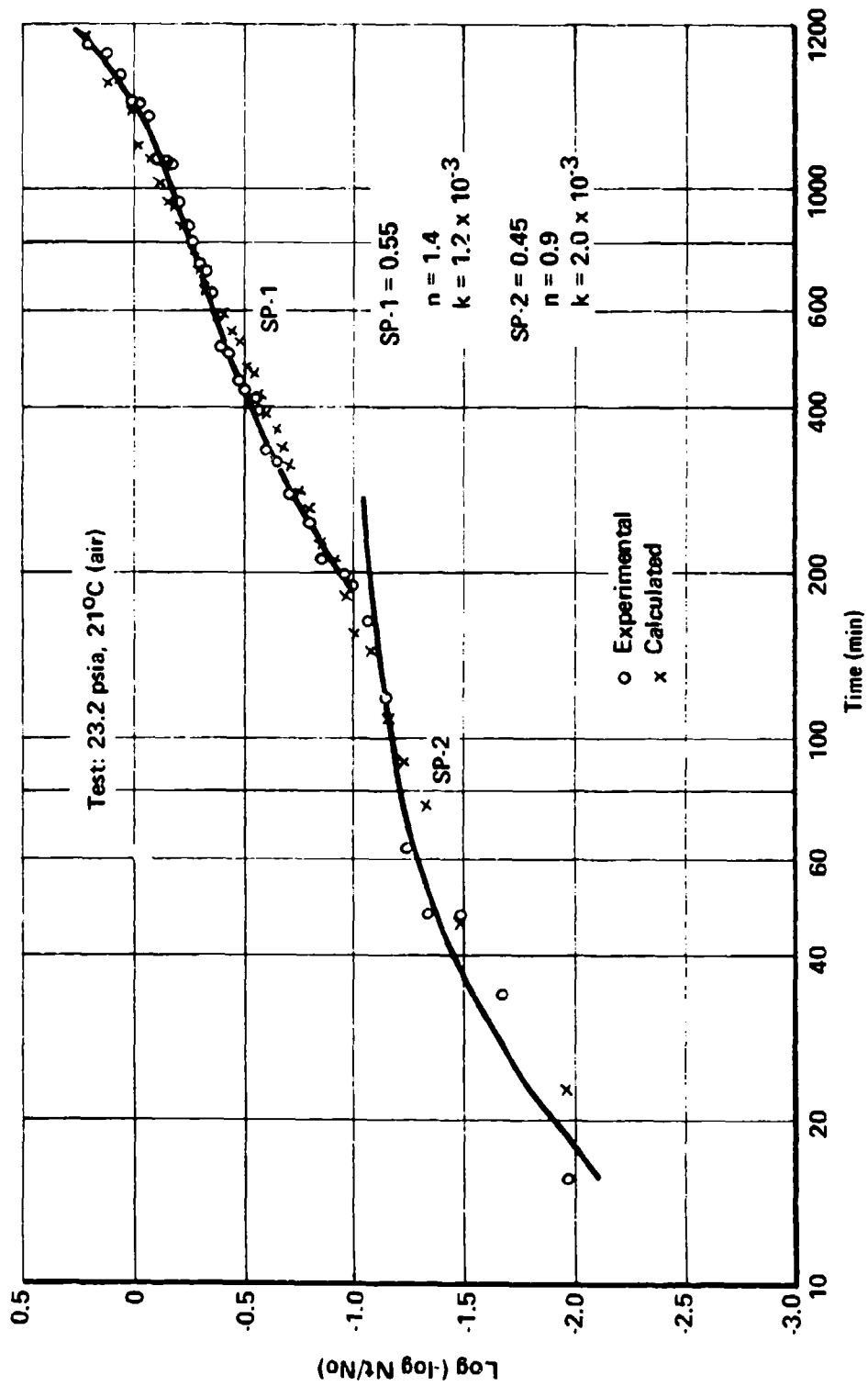

Figure 3-19 Ballistically Optimized PCDF Propellant Aged 22 Days at 40°C

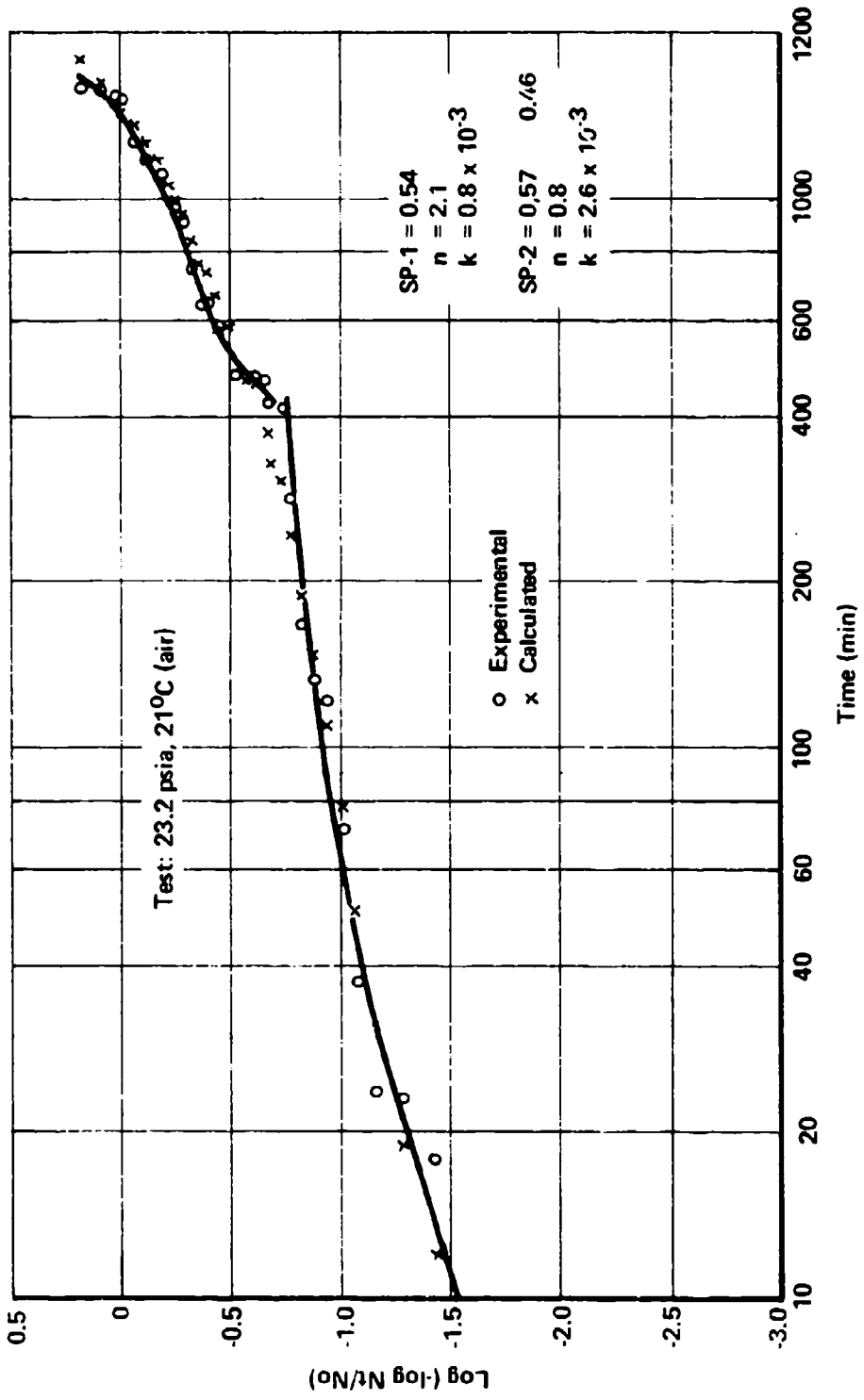

Figure 3-20 Ballistically Optimized PCDE Propellant Aged 30 Days at 40°C

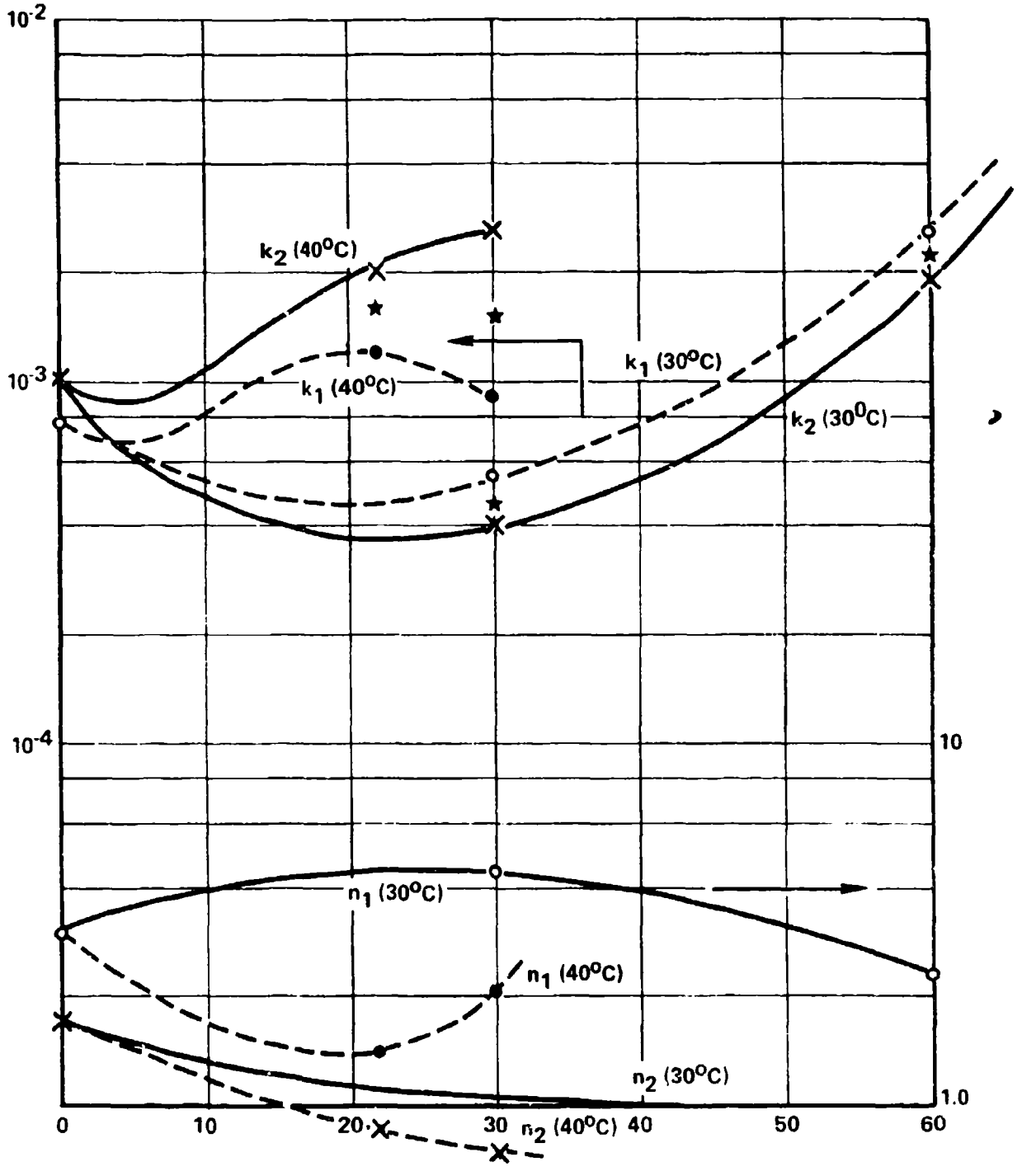

Figure 3-21 Ballistically Optimized PCDE Propellant, 30°C Aging

At 30°C this propellant appears to undergo post-cure during the initial 30 days storage which is indicated by a decrease in the rate parameters k_1 and k_2. After 30 days the binder appears to suffer degradation to cause the values for k to increase markedly. At 40°C the post-cure period was too short to be observed (first data points after 22 days storage). Beyond this period the data grossly resemble the 40°C aging data for the model propellant, namely a period of binder softening to increase the k-values, followed, in turn, by a reversal suggesting a secondary crosslink process. The stars in Figure 3-21 denote failure by X-ray. With the exception of the 30 days at 30°C failure point (1 specimen) the failures appear to fall within the periods of increasing k-values (softening), and the data suggest that it is the combination of high initial gassing rates (Figure 3-17) and binder softening during this time period that renders the propellant susceptible to failure.

Figure 3-22 shows calculated failure frequencies for groups of 1000 test specimens maintained under 23 psia, 30°C after 30 days aging at 30 and 40°C. The data show that aging has a much more pronounced effect upon failure distribution than is indicated by the uniaxial tensile test data (Table 3-11).

Kinetic Analysis of Constant Strain Rate Tensile Data. Figure 3-23 gives a plot of the temperature corrected failure times under constant strain rate and constant load. It is noted that the constant-load data deviate from the constant strain rate data, and in this regard this propellant differs from both the model PCDE and the AlH /TVOPA propellants. The discrepancy persists even if the constant strain rate data are transformed into constant load data using Equation 10, it implies that

$$t_\sigma = \int_0^{t_{\dot\epsilon}} \left(\frac{\sigma_{(t)} - \sigma_{(\infty)}}{\sigma(t_{\dot\epsilon}) - \sigma_{(\infty)}} \right)^\eta dt \qquad (10)$$

the stress-time shift factors, a_σ, are not the same. Non-linearity also is indicated by the change in the exponent, η, upon increasing the load from 23 psia to 30 psia in the constant load creep failure test (Table 3-12).

Table 3-13 quotes the parameters for the shift factors that were derived from the constant strain rate tensile data, and it compares these data with the values derived from the constant load creep failure tests. The data show reasonably good agreement with regard to $\sigma_{o(\infty)}$, but poor agreement with regard to the k-values.

Figure 3-24 shows the effect of aging at 30°C upon the long-term stress, these data are compatible with the data presented in Table 3-13 in so far as $\sigma_{o(\infty)}$ decreases as the k-values increase, either set of data indicating polymer network degradation. There was too much data scatter to derive meaningful information for the effect of 40°C aging upon $\sigma_{o(\infty)}$, and the effect of both 30 and 40°C aging upon binder network moduli.

Burn Rates. The burn rates were determined as a function of aging time at 30°C. The data (Table 3-14) show a small decrease after 60 days aging.

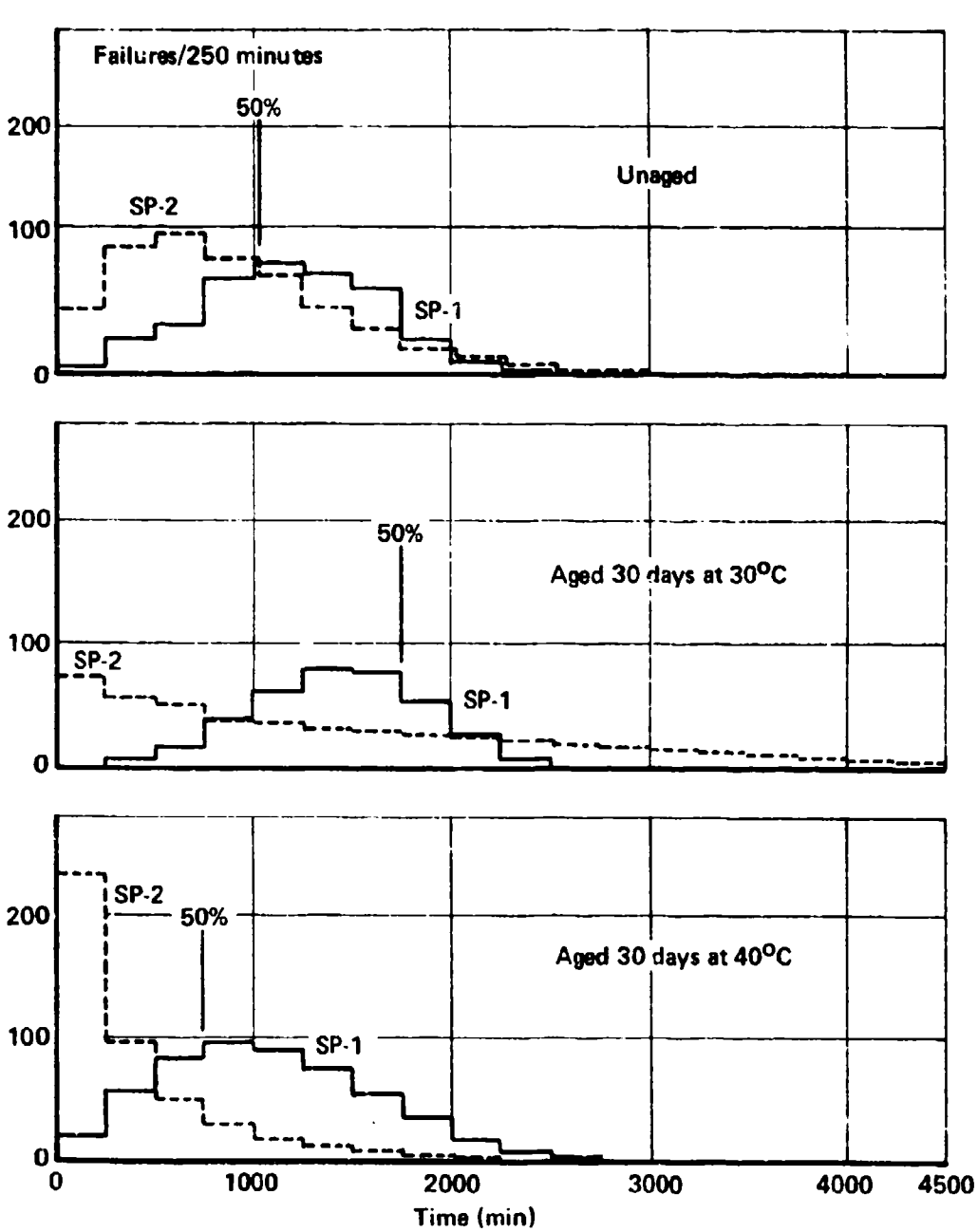

Figure 3-22 Ballistically Optimized PCDE Propellant - Calculated Failure Frequencies, 1000 Test Samples 23.2 psia, 21°C

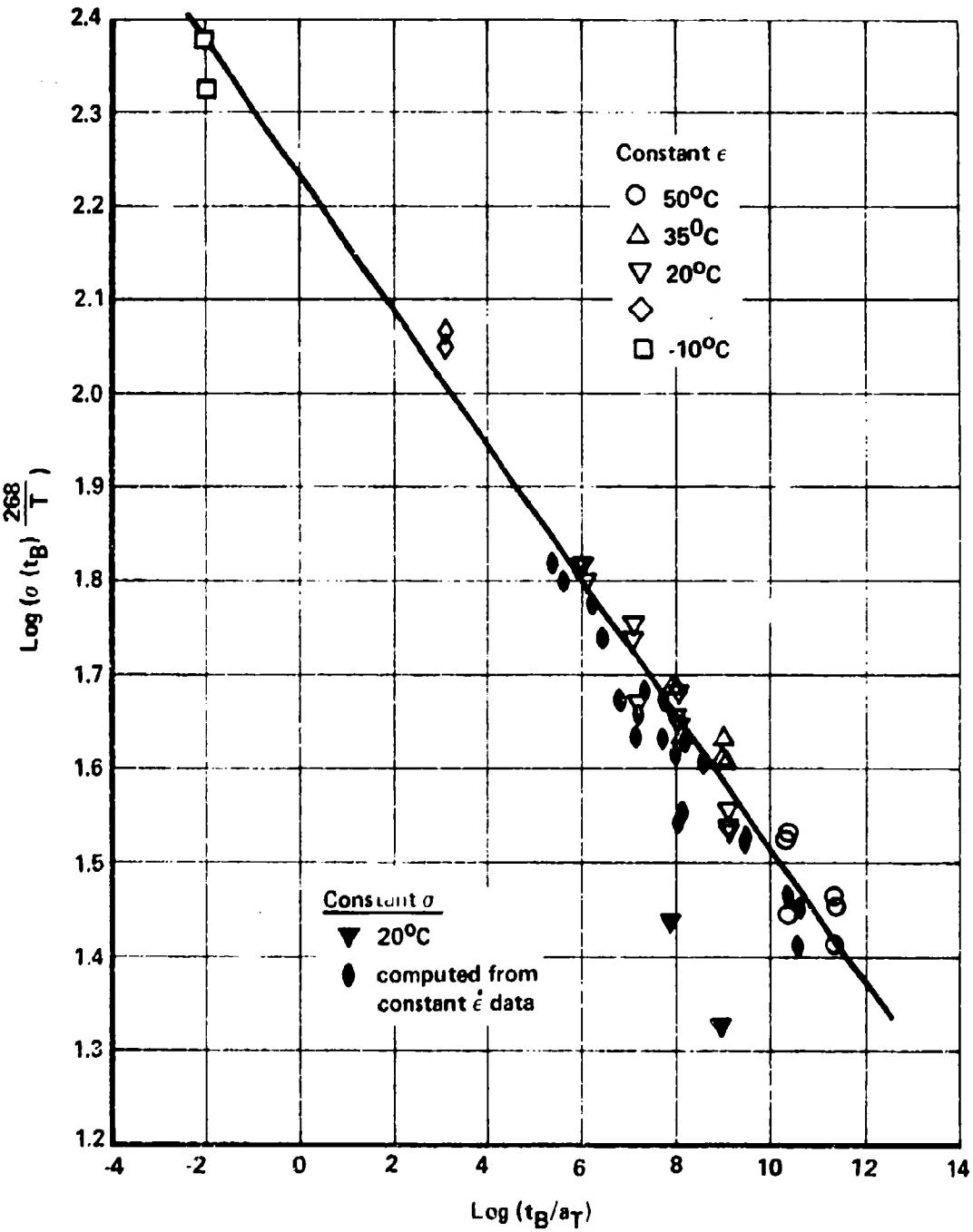

Figure 3-23 PCDE Active Propellant, No. 73-05-245, Master Failure Curve.

Table 3-13

DATA COMPARISON, CONSTANT STRAIN RATE VERSUS CONSTANT LOAD, UNAGED PROPELLANT

(a) Constant Strain Rate Data

$k_o = 18.2 \pm 3.2$ Temperature Range: 20 - 50°C

$n = 0.93 \pm 0.22$ Strain Rates: 0.108 - 0.000108 min^{-1}

Stress-Time Shift Factor

$\sigma_{o(\infty)} = 17.8$ psia

$\sigma_{o(1)} = (63,406$ psia)

$\eta = 2.861$

Temperature-Time Shift Factor

$$\log a_T = - \frac{16.51\ (T - 268)}{43.95 + T - 268}$$

Strain Rate Shift Factor

$a_{\dot{\epsilon}_o} = 1.991 \times 10^{-9}$

(b) Constant Load Creep Failure Data

Time-to-Failure 50% Point Minutes, at	Time-to-Failure, 50% Points, Minutes		
	Composite	Sub-Population 1	Sub-Population 2
23.2 psia Load	930	1164	806
30 psia	85	58	133
$a = \frac{t_b(30)}{t_b(23.2)}$	0.091	0.050	0.165
$\sigma_{o(\infty)}$, psia	16.2	17.6	18.6

(c) Calculated Rate Constant, $k_{(\sigma, T)}$ Using Constant Strain Rate Data

	Calculated $k_{(\sigma, T)}$	Values Derived From Constant Load Creep Failure Tests
23.2 psia	1.47×10^{-4}	k_1 7.6×10^{-4}
		k_2 1×10^{-3}
30 psia	1.5×10^{-3}	k_1 1.4×10^{-2}
		k_2 5.2×10^{-3}

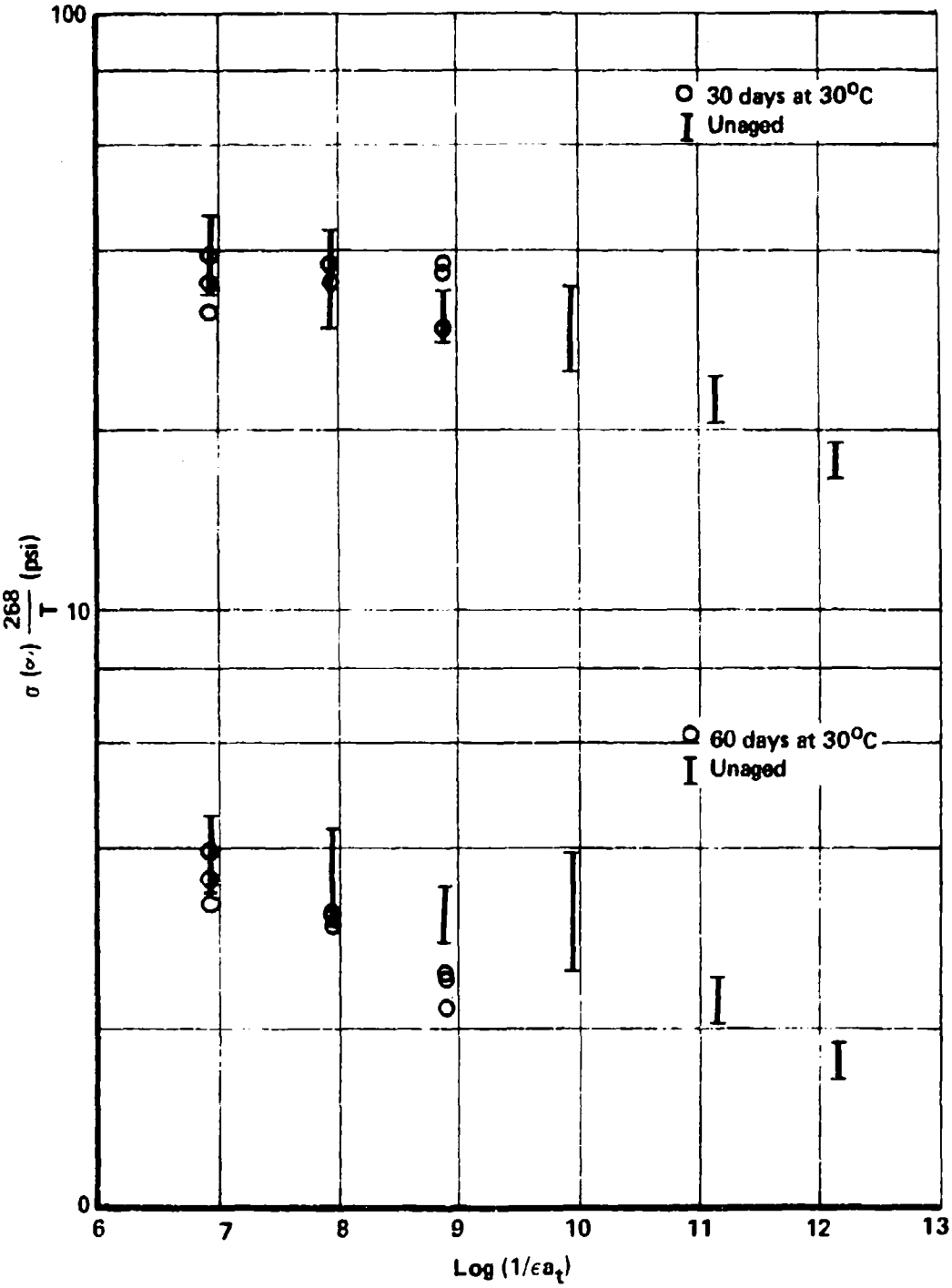

Figure 3-24 Long-Term Stress of Aged PCDE Active Propellant, No. 73-05-245.

Table 3-14

BALLISTIC PROPERTIES OF UNAGED AND AGED PCDE ACTIVE PROPELLANT, NO. 73-05-245

Burning Rates at 21°C

Sample	Pressure 750 psi	1,000 psi	1,200 psi
Unaged, in./sec	0.379	0.448	0.511
	0.373	0.456	0.503
Average	0.376	0.452	0.510
Aged 30 days at 30°C, in./sec	0.376	0.454	0.515
	0.378	0.461	0.524
Average	0.377	0.458	0.520
Aged 60 days at 30°C, in./sec	0.353	0.457	0.494
	0.352	0.445	0.498
	0.352	0.443	0.496
Average	0.352	0.448	0.496

3.2.2.3 PCDE Propellants, Summary

The most noteworthy observation with the model and the ballistically optimized PCDE propellants is a reversal of the aging effect after relatively short storage periods at temperatures in excess of 30°C. This effect is not likely to be associated with a normal post-cure process; it seems to involve a secondary chemical crosslink process involving some peculiarity of the polymer's structure.

This secondary cross-link process seems to operate with a relatively high activation energy to cause it to be insignificant at 30°C but pronounced at 40 to 50°C. The surveillance periods with either propellant were too short to determine, however, whether this process continues for extended time periods to produce a shelf-life limitation because of excessive hardening.

The model PCDE propellant survived 181 days aging at 50°C, none of the test specimens revealing cracks by X-ray after this aging period. The ballistically optimized PCDE propellant, however, failed by cracking after comparatively brief storage periods at both 30 and 40°C. This is attributed to a relatively high initial rate of gas generation occurring at a time where the binder appears to soften to render the system highly sensitive to internal gas pressure. The fact that gas generation rates level off after this initial period suggests that instability is attributable to residual polymer structural irregularities.

Both propellants afford bimodal distributions in the constant-load creep failure test which is an indication that the systems are not uniform. The data are not sufficient, however, to state whether this is attributable to processing, or an inherent polymer or propellant property.

A more direct comparison between the two propellants is rendered difficult by the fact that different polymer lots were used. A polymer lot-to-lot difference, for example, could account for the observation that aging of the model propellant has a grossly similar effect upon tensile properties and constant-load creep failure behavior, while the two sets of data are at odds with the ballistically optimized system. This, in turn, might be attributed to lot-to-lot differences in polymer functionality that could translate into significant differences in polymer network properties. It is noteworthy in this regard that the polymer network strain capability of the AlH_3/TVOPA propellant, which uses a polymer of reasonably close controlled functionality, is strain rate insensitive, while the polymer network strain capability of the PCDE propellants is distinctly strain rate sensitive. It suggests that entanglement of the nonlinear PCDE polymer plays an equal or greater role than chemical crosslinking in providing stress capability.

If these interpretations are correct, then one is led to conclude that the polymer used in the Aerojet propellant was deficient in quality relative to the material used in the model propellant.

(The reverse is blank)

4. RECOMMENDATIONS

4.1 PCDE PROPELLANTS

This investigation has produced evidence that thermal stability problems with PCDE propellants are attributable to impurities or structural irregularities in the PCDE prepolymer, and that efforts to produce thermally stable propellants must concentrate upon upgrading the quality of this prepolymer. There further is evidence for variability in prepolymer functionality that may have a significant effect upon propellant mechanical properties and aging life.

Data produced under this program also confirm earlier observations regarding a suspected nitrate ester plasticizer interference in the cure process to cause the curative to be utilized ineffectively.

The model propellant data, and to a lesser extent the data produced with the ballistically optimized PCDE propellant, furnish evidence for a secondary cure or crosslink process. There is reason to suspect that this process is peculiar to the structure of the PCDE polymer, and since it could result in considerable and uncontrollable hardening of the propellant further more detailed studies are clearly warranted.

4.2 METHODS DEVELOPMENT

With few, if any exception, propellant and motor development programs aim to improve ballistic performance as a means to reduce system cost while maintaining or increasing payload or range capability. There has been large emphasis upon the evaluation of various means of increasing density specific impulse, the controllable range of interior ballistic properties, and efficiency in the manufacture of motors. There persist difficulties, however, in arriving at realistic assessments of motor replacement requirements, and this difficulty can translate into large uncertainties in forecasting life cycle cost. It may have a particularly critical impact where in order to reduce projected life cycle cost performance is increased possibly at the expense of service life.

There particularly exists a need to establish test and analysis methodology to provide an early assessment of a new propellant's or motor's service life capability while the system is under development, and to allow service life capability to be placed on equal footing with ballistic performance in establishing development objectives. The methods that have commonly been

used generally provide such information after the fact so to be of limited practical value. There equally remains a need to establish test and analysis methodology that enables material, formulation and processing variables that may affect service life to be better controlled during manufacture.

There has been a tendency for programs, contractors or agencies to concentrate upon some specific aspect of the problem, or to rely heavily upon some specific approach. It is to be realized that "service life" constitutes a statistical concept that must incorporate and account for the mechanical as well as chemical components of the problem, and there must be better recognition of the distinction between a systems inherent service life capability, under some defined temperature-load-time conditions, and an inventory's actual service life under widely varying field conditions. There exists technology today that, if properly implemented, can be used to assess and control service life capability, while actual service life predictions for inventories under field conditions may always remain difficult to accomplish.

This program tested an approach that constitutes a modification of Aerojet's Cumulative Damage analysis concept, and that is based on Weibull survival probability statistics. This approach, as originally formulated by Halpin at the Air Force Mayerials Laboratory, appears to have considerable merit for assessing, and ultimately controlling, propellant service life capability. The approach accounts for the statistical nature of the failure process, and it provides a means to assess and forecast the effects of chemical aging upon failure distributions. It accomplishes this by defining the distribution of failures in terms that have physico-chemical significance, thereby providing a bridge for relating the statistical element to propellant compositional and structural factors; it further relies upon well established principles to allow test data extrapolation from laboratory to real time conditions.

Though the results that were obtained in implementing this approach with AlH_3/TVOPA, PCDE and standard composite propellants, both unaged and aged, were encouraging, they nevertheless revealed need for resolving various difficulties in data analysis, interpretation and extrapolation.

There commonly is a tendency to implement a method that carries promise in an effort to produce practical results without having expended the necessary effort to fully master the method. This produces unsatisfactory results and disappointment, and it can lead to the premature abandonment of what might have been a good and rational approach to a major problem.

As stated earlier, the approach relied upon by LPC under this program is not a new approach; it constitutes a modification, extension and combination of efforts and approaches pursued by other laboratories within industry and government. The merit of the work done by LPC is considered to rest with the demonstration that the various prior efforts are not in conflict or competition, but that they constitute integral parts of a common approach, and that this approach combining the chemical, mechanical, and statistical

aspects merits further attention and support. The specific areas that, in Lockheed Propulsion Company's assessment, now require further attention are as follows:

The data that were obtained in implementing the Halpin survival probability approach with a broad variety of composite propellants evidence that in all cases the constant-load fatigue life (creep failure distribution) can be defined by an expanded Weibull survival probability function

$$N(t)/No = \alpha_1 \exp -(k_1 t)^{n_1} + \alpha_2 \exp -(k_2 t)^{n_2}$$

$$\text{where:} \quad k = \frac{k_o}{a_T{}^d a_\sigma a_C}$$

It implies that the constant-load fatigue life, under any given condition with respect to temperature and load, can be defined by determining the number distribution of specimens among two sub-populations (α_1, α_2), and the scale (k_1, k_2) and shape (n_1, n_2) parameters for the sub-populations. Experience further shows that with specific exceptions $k_1 = k_2$ as might be expected.

To afford practical significance to the data, means must be provided to extrapolate the test data from quick time test to real time motor conditions, to account for chemical aging, and to account for cyclic loading.

Data extrapolation from quick-time test to real-time motor conditions is accomplished, in principle, using the temperature-time shift factor, a_T, and the load-time shift factor, a_σ. The numerical values for the temperature-time shift factor can be derived from uniaxial tensile data relying upon the WLF temperature-time superposition principle. There persist difficulties, however in determining the numerical values for the load-time shift factor, a_σ, the latter requiring knowledge of the values for the long term stress, $\sigma_o(\infty)$, and the exponent, η, of Ferry's power law. The data that were obtained provide some evidence that the exponent, η, may be a constant approaching 2.67, which, if found to be true, would simplify matters and reduce the problem to determining the value for $\sigma_o(\infty)$.

Aerojet assumed that $\sigma_o(\infty)$ for propellants approaches zero. This may, or may not be correct; LPC data in superimposing creep-failure data suggest that $\sigma_o(\infty) \neq 0$ if the system is adequately crosslinked. However, the LPC evidence is based upon creep failure data obtained over a limited range of loads only, and upon the kinetic analysis of constant strain rate tensile data, the latter method requiring significant data extrapolation.

It appears necessary, therefore, to concentrate efforts upon establishing better means for determining $\sigma_o(\infty)$ as a function of propellant gel content or effective crosslink density. One may add, at this point, that non-linearity in load-time superposition may be attributable to differences in the values for the long term stress for the sub-populations.

Chemical aging reflects in a change in the values for the scale parameters, k, and there is some evidence that the rate of change in the k-values as a function of storage life at some temperature may be predicted using chemical rate expressions that define the change in gel content as a function of zero-time properties and aging time. More importantly, however, may be the chemical aging induced changes in the shape parameters for the sub-populations.

There is reason to assume that the shape parameters, n, constitute composite quantities to reflect both internal stress fields and physical defect size distribution. Judging from the available data any process that causes physical damages appears to reflect in an increase in the value(s) for n. These processes include mishandling (e.g. bending) of the test specimens, internal gas generation to cause voids or cracks (AlH_3/TVOPA propellants), and chemical aging possibly by impairing binder-AP bond integrity.

There does not as yet exist a basis for rationalizing the changes in n as a function of aging time under given temperature-load-time histories, and graphical data extrapolation presently constitutes the only means of forecasting beyond actual periods of observation. There is reason to expect, however, that the time-temperature-load dependent changes in n-values are predetermined by propellant compositional factors (e.g. particle size and agglomerate size distributions), and dependent upon chemical events (internal gassing, changes in gel content) that can be assessed independently. What appears necessary here is an aging study using model propellants varying in solids loading and solids particle size distribution, zero-time gel content and bonding agents.

It further may be argued—and there is rather limited experimental evidence to support it—that all of the critical parameters (k_j, n_j, $\sigma_o(\infty)$) are interdependent, and that the chemical aging induced changes can all be related to common causes, i.e. chemical aging induced changes in basic physico-chemical properties. It is in this area where Kaelble's kinetic analysis upon further elaboration and refinement is expected to contribute significantly toward providing the scientific rationale for relating cause and effect.

There exists the additional problem of quantifying the effects of cyclic loading, and a review of Halpin's data as well as LPC data suggests that this problem may not be as difficult as has frequently been assumed. Subjecting a series of tensile specimens to a single load cycle has been shown to inflict physical damage, and to result in the appearance of a sub-population having a higher n value. Repetitive loading to levels above some critical load, appears to reflect in the transfer of specimens into the sub-population having a higher n-value. This transfer may be complete after a given number of cycles to restore a uni-modal distribution with $k = k'$ and $n' > n$, where k' and n' represent the Weibull parameters of the system having undergone cycling. It implies that upon cycling a propellant between constant stress or strain levels, the system may initially be cycle sensitive but become temperature-time-load sensitive after the cavitation process has gone to completion.

In conclusion, it appears that by combining the chemical aging oriented approach with Halpin's statistical cumulative damage approach, and by further relying upon Kaelble's kinetic analysis, it will indeed be possible to provide a practical means of defining propellant-in-motor service life capability on the basis of quick-time laboratory test procedures. One may further expect that related analysis and test methods can be standardized to the point where "service life capability", as a propellant quality criterion, can be placed on equal footing with other specifications relating to mechanical properties, ballistic properties and interior ballistic properties.

(The reverse is blank)

5. REFERENCES

3.1 D.A. Willoughby, E.L. Allen, J.E. Engle, and J.F. Fulton, A Small Scale Fissuring Test, Rohm and Haas Company, Report No. S-227, September 1969.

3.2 J.C. Halpin and H.W. Polley, Observations of the Fracture of Viscoelastic Bodies, J. Composite Materials, 1, 64-81 (1967).

3.3 D.H. Kaelble, E.H. Cirlin, and M. Shen, Interfacial Morphology and Autohesion of A-B-A Triblock Copolymers, COLLOIDAL AND MORPHOLOGICAL BEHAVIOR OF BLOCK AND GRAFT COPOLYMERS, C.E. Molau Editor, Plenum Press, New York, 1971.

3.4 Lockheed Propulsion Company, Aluminum Hydride Propellant Shelflife: Interim Technical Report No. 532-I-1, January 1972 (CONFIDENTIAL); Interim Technical Report No. 532-I-2, April 1972 (CONFIDENTIAL); Interim Technical Report No. 532-I-3, August 1972 (CONFIDENTIAL).

(The reverse is blank)

Appendix A

Propellant shelflife and motor service life constitute statistical concepts, and methods that define these quantities in terms of projected failure distributions as a function of given time-temperature-stress-strain histories must be relied upon.

This program evaluated two statistical approaches, namely Halpin's approach based upon the analysis and interpretation of constant-load fatigue (creep failure) test data, and Kaelble's approach based upon a more detailed analysis of constant strain rate tensile data. The application of these methods for determining the aging characteristics and resulting effects upon either distribution of constant-stress time or constant strain rate failure time of AlH_3/TVOPA and PCDE propellants was reviewed in Sections 3 and 4. This part of the report centers more upon the methods themselves and problems that were encountered in applying them, with emphasis upon Kaelble's analysis of constant strain rate tensile data.

A.1 GENERAL

Both methods are based upon the concept that rubbers or composites contain a very large number of original defects, and that failure results if one or more of these defects under the influence of an applied stress attain a critical size. The distribution of failures under a given temperature-stress regime thereby reflects the defect size distribution.

Halpin's definition of the cumulative distribution of failure function, based upon the assumption of a linear crack growth rate, was reviewed in Section 3, and elaborations can be found in the quoted references. The results obtained in applying this method toward defining the service life capability of propellants in the form of motor grains were summarized in Section 4. The following summarizes specific observations made under this program, and in applying the method with SRAM, TP-H1011 and ANB-3066 polybutadiene based propellants.

A.1.1 General Experience in applying Halpin's Cumulative Damage Approach

Various of the propellants studied afforded uni-modal distributions with the freshly processed or cold-stored systems, but multi-modal distributions as the propellants progressively aged. It implies that the linear cumulative damage concept is not generally applicable. It further

implies that the effect of the chemical aging process upon the distribution of failures cannot be defined by introduction of a chemical shift factor, a_C, as suggested by Halpin. Instead, the aging effect must be defined by determining the chemical aging induced changes on the Weibull parameters of each sub-population to produce predictions by graphic extrapolation.

With the exception of the ballistically optimized PCDE propellant, the creep-failure data obtained at different loads could be superimposed using Halpin's stress-time shift factor, a_σ, obtained from constant strain rate data. However, in all cases data were available over a rather limited range of applied loads only; this leaves uncertainty whether linearity is retained in extrapolating to load levels approaching, or falling below, the long term stress, $\sigma_o(\infty)$. Aerojet assumed that for most propellants $\sigma_o(\infty)$ is equal to or approaches zero. This might be argued, for example, by quoting the Zhurkov temperature-load equivalence which LPC has shown to be valid for CTPB propellants using time-of-flight dynamic mass spectrometer methods. Nevertheless, this remains an argument that requires further attention.

As suggested by Halpin, the rate parameter(s), k, appear to reflect a polymer property, and data obtained with TP-H1011 propellant give some indication that k is directly related to binder gel content. If further work should confirm this, then the rate of change of the scale parameter(s) k as a function of temperature and time can be predicted using chemical rate equations that define the change in gel content with aging. It was found that with specific exceptions the k-values for sub-populations are identical within experimental errors. Notable exceptions were the ballistically optimized PCDE propellant, and a propellant that contained soft polymer gel particles within an otherwise adequately cured polymer matrix. The data further suggest that the rates of change of the scale parameter(s) k, the binder network modulus E_{m_2} and the long term stress $\sigma_o(\infty)$ are interrelated, all possibly being some function of binder gel content.

A more difficult problem exists in interpreting the physical-chemical significance of the shape parameter(s), n. Halpin postulates that the shape parameter, n, reflects the dimensionality of the defect growth process, a uniaxial stress field to afford a shape parameters of n = 1.0, a tri-axial stress field to afford a shape parameter of n = 3. The data that were obtained under this and other programs suggest that n in fact is a composite figure to reflect both internal stress fields and defect size distribution. Any process that may be presumed to inflict physical damage appears to reflect in an increase in the value(s) for n. These processes include gas void formation (AlH_3/TVOPA propellants), break-up of AP agglomerates (composite propellants) and aging induced particle dewetting. There presently does not seem to exist a valid theoretical basis for predicting chemical aging induced changes in the n-values, and an empirical extrapolation of data must presently be resorted to (see Figures 4-10 and 4-11, Section 4). The statistical significance of n rests with the definition of the shape of the failure distribution curve; this can have sizeable practical consequences.

One may state in summary that the Halpin statistical cumulative damage approach appears applicable with propellants, and that by using the expanded

form of the Halpin survival distribution function to account for non-uniformity one is provided with a means to account for chemical aging effects that cause the system to be no longer amenable to analysis using linear cumulative damage concepts. Halpin's approach offers the further advantage of relative simplicity in implementing it in the laboratory, and in the analysis and interpretation of the data.

A.1.2 General Experience In Applying Kaelble's Analysis Of Constant Strain Rate Tensile Data

The uniaxial tensile test is used widely for the purpose of defining and controlling propellant mechanical properties even though there is apprehension regarding reliance upon these data in assessing propellant mechanical response in motors. Kaelble, in developing his kinetic analysis concept, assumed the attitude that the fault rests less with the test itself, but a lack of sophistication in the analysis and interpretation of the test data. The results that were obtained under this and parallel programs at LPC, wherein Kaelble's approach was applied with propellants, show that this attitude has merit.

A step-by-step description of Kaelble kinetic analysis of constant strain tensile data is given under Subsection A.2. The following provides a general summary of the test experience in applying this approach with AlH_3/TVOPA, TVOPA, PBAN and CTPB propellants.

Kaelble's contention was that the constant strain rate tensile data contain all information necessary to define constant-load creep failure distributions by equating the "Damage Function" $B(\epsilon,t)$ with the Halpin survival probability function. Experience in applying this analysis approach with propellants indicates that this is not necessarily correct, possibly because of solid filler effects. Propellants constitute very weakly crosslinked viscoelastic systems with much of the stress capability being provided by the filler reenforcing action. This reenforcing action, in turn, is dependent upon the quality of the binder-filler bond, and it is a well established fact that the mechanizm of bond failure is highly strain- or peel-rate sensitive. High strain- or peel rates may cause cohesive failure within the polymer phase, while low peel rates may cause adhesive failure. As a result, and unless the binder-filler bond is quite poor, the constant strain rate data may be somewhat more indicative of binder properties, while the constant-load creep failure test data may be more indicative of the properties of the composite. This seems compatible with the observation that the Kaelble analysis affords k-values that are in reasonable agreement with the results of the Halpin analyses, while there exist large discrepancies in the values for the shape parameter(s), n. This, in turn, could be a consequence of the analysis methods that were used, and that ignored the cavitation process to equate the Halpin survival probability function strictly with the Damage Function of the defect growth process. It is conceivable, therefore, that further refinements in the data analysis and treatment might overcome this shortcoming. In its present state of development, however, Kaelble's kinetic analysis, as applied to propellant uniaxial tensile data, cannot be

used to define constant-load failure distributions because of inability to produce the correct values for the shape parameters, and inability to distinguish between sub-populations.

This does not detract from the method's merits as a diagnostic tool, and as an expedient to derive the parameters of the temperature-time and stress-time shift factors.

The kinetic analysis provides a means to analytically isolate the cavitation and the defect growth processes, and data produced with HTPB propellants show that this distinction can be of considerable interest in evaluating bonding agents and associated chemical aging effects. Analytical isolation of the defect growth process further enables polymer network properties to be defined. This provides a means to determine whether an aging induced change in mechanical properties is attributable to a change in bulk binder proerties, or attributable to changes within the binder-filler boundary layers.

In view of the above Kaelble's kinetic analysis of propellant constant strain rate tensile data may be viewed to be a complimentary analysis method, but not a substitute for the Halpin method.

A.2 KINETIC ANALYSIS OF CONSTANT STRAIN RATE TENSILE DATA

If a viscoelastic material is subjected to a constant strain rate tensile, and if the data are plotted in terms of $\lambda^2(\lambda = \epsilon + 1)$ versus ϵ/σ, then a data plot as schematized in Figure A-1 is obtained. On the application of strain, deformation of propellant occurs described by the modulus E_{m_1} and ultimate extensibility λ_{m_1}. This is followed by stress relaxation due to cavitation described by the damage function $B_1(\epsilon, t)$. After cavitation has ceased, orientation of the binder network occurs described by the network modulus E_{m_2} and the ultimate extensibility λ_{m_2}. Eventually, the defects or cracks start to grow. This process is described by the damage function $B_2(\epsilon, t)$. The final result of crack growth is fracture of the test specimen.

In molecular theory, nonlinear viscoelasticity is described by the approximate constitutive equation A-1. Treloar has shown that large deformation of rubbers can be adequately described by taking the inverse Langevin function for the strain function

$$\sigma = f(\epsilon)\epsilon(t) \qquad \text{(A-1)}$$

$f(\epsilon)$. Kaelble has taken the following simple function which is a very good approximation to the inverse Langevin function. The ultimate extensibility, λ_m is directly

$$f(\epsilon) = \frac{1}{1 - \lambda^2/\lambda_m^2} \qquad \text{(A-2)}$$

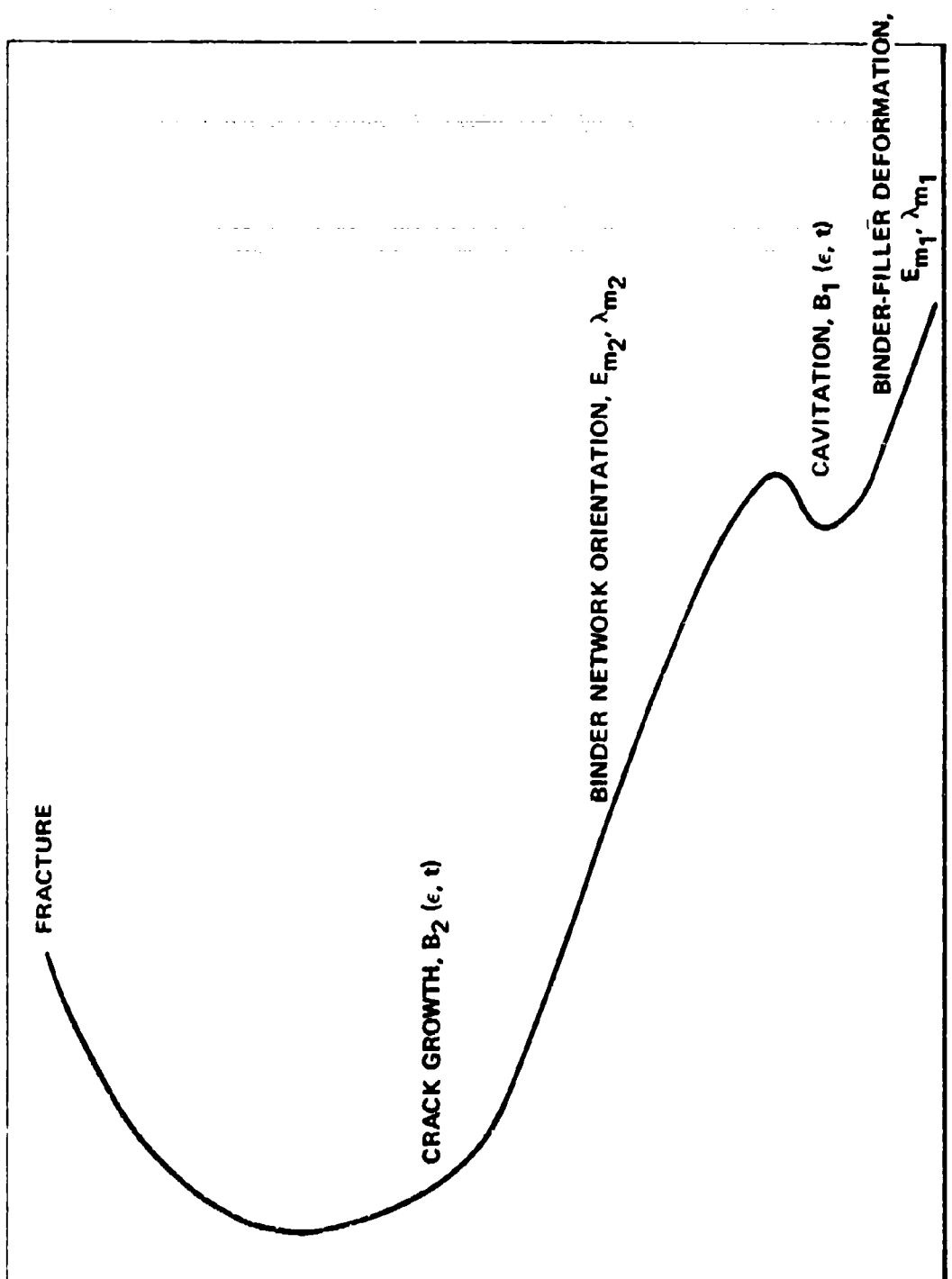

Figure A-1 Idealized Curve of λ^2 versus ϵ/σ Illustrating the Kinetic Mechanism of Failure of a Solid Propellant

related to the number average bonds between effective crosslinks. By substituting equation A-2 into A-1, the constitutive equation (A-3) for an elastomer is obtained.

$$\sigma = \epsilon \frac{E_m(t)}{1-\lambda^2/\lambda_m^2} \qquad \text{(A-3)}$$

If an elastomer sustains damage, the stress response falls below that predicted by Equation A-3 (Figure A-2), and Kaelble accounts for this deviation from ideal behavior by introducing a "Damage Function", $B(\epsilon, t)$, (Equation A-4):

$$\sigma = \epsilon \frac{E_m(t)}{1-\lambda^2/\lambda_m^2} B(\epsilon, t) \qquad \text{(A-4)}$$

Kaelble, upon applying this analysis concept with Kraton block-polymers, showed that this damage function, as defined by rearranging Equation A-4

$$B(\epsilon, t) = \frac{\sigma}{\epsilon} \frac{1-\lambda^2/\lambda_m^2}{E_m(t)} = \exp - \left(\frac{kt}{a_\sigma a_T a_\epsilon}\right)^n \qquad \text{(A-5)}$$

can be equated with Halpin's survival probability function (Equation A-5).

LPC, in implementing this approach with propellants, observed the following:

(a) With unaged propellants failure commonly is observed to occur via a two step process, namely a cavitation step followed by a crack growth or tear process, and analysis of the data generally affords two damage functions (Figure A-1):

- Cavitation Step

$$\text{Damage Function} = B_1(\epsilon, t) = \frac{\sigma}{\epsilon} \frac{1-\lambda^2/\lambda^2_{m_1}}{E_{m_1}(t)}$$

where:

λ_{m_1} is the ultimate extensibility of the system in the absence of cavitation or tear processes

E_{m_1} is the composite modulus prior to the occurrence of cavitation or tear damages

σ_{cr_1} is the critical stress for the cavitation step, i.e. the stress level at which the system starts to deviate from ideal behavior

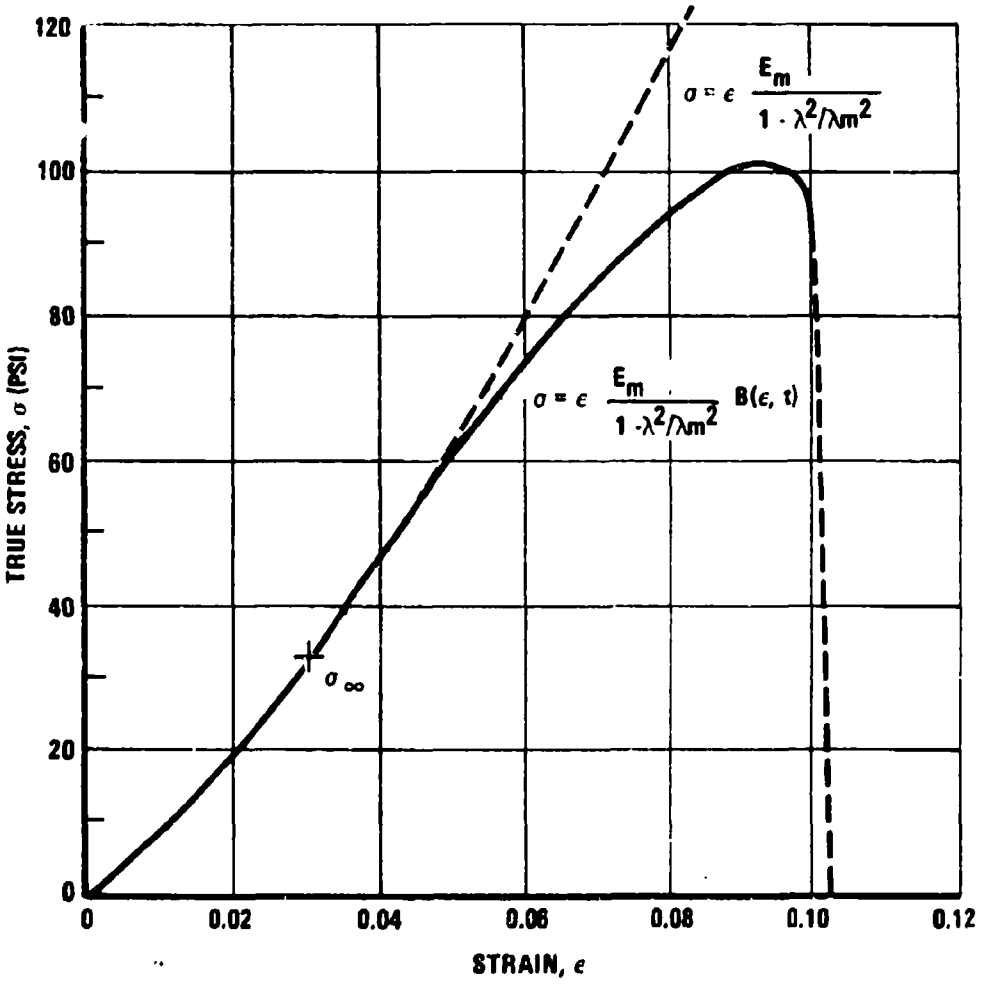

Figure A-2 Kaelble's Damage Function Elastomers

- Crack Growth Step

$$\text{Damage Function} = B_2(\epsilon, t) = \frac{\sigma}{\epsilon} \frac{1 - \lambda^2/\lambda^2_{m_2}}{E_{m_2}(t)}$$

where λ_{m_2} is the ultimate extensibility of the binder network in the absence of tear damages

E_{m_2} is the binder network modulus, again, ignoring tear damages

σ_{cr_2} is the critical stress for the crack growth or tear process, i.e. the stress level at which the systems start to deviate from ideal behavior ($B_2 \leq 1.0$)

The values for σ_{cr_2} are temperature and strain rate sensitive, and by analyzing test data obtained over a broad range of temperatures and strain rates, the normalized value for the long term stress, $\sigma_o(\infty)$, is obtained by graphic extrapolation.

(b) In attempting to equate Kaelble's damage function, $B(\epsilon, t)$, with Halpin's survival probability function in accordance with Equation A-5, reasonable agreement was obtained with regard to the k-values using the damage function for the crack growth step ($B_2(\epsilon, t)$); this is compatible with Halpin's original concept, namely that the scale parameter, k, represents the linear crack growth rate constant. On the other hand, Kaelble's kinetic analysis of the constant strain rate tensile data commonly yielded values approaching 1.0 for the shape parameters, n, even with systems where the constant-load creep failure tests afforded significantly higher values. The Kaelble analysis, moreover, is not applicable to determining the survival probability function of systems affording multi-modal failure distributions.

(c) With propellants that have undergone chemical aging, the cavitation step (Figure A-1) may no longer be identifiable.

In view of this general experience the following conclusions appear warranted.

(1) Kaelble's kinetic analysis of constant strain rate tensile data cannot be relied upon to define propellant constant-load creep failure behavior in terms of the Halpin survival probability function.

(2) The kinetic analysis nevertheless provides valuable information by rationalizing propellant mechanical behavior in physico-chemical terms that can be related with propellant composition and structure It thereby enhances the value to be derived from the commonly performed tensile tests.